Accepted Manuscript

Particle fluxes and their drivers in the Avilés submarine canyon and adjacent slope, central Cantabrian margin, Bay of Biscay

A. Rumín-Caparrós, A. Sànchez-Vidal, C. González-Pola, G. Lastras, A. Calafat, M. Canals

Please cite this article as: Rumín-Caparrós, A., Sànchez-Vidal, A., González-Pola, C., Lastras, G., Calafat, A., Canals, M., Particle fluxes and their drivers in the Avilés submarine canyon and adjacent slope, central Cantabrian margin, Bay of Biscay, *Progress in Oceanography* (2016), doi: http://dx.doi.org/10.1016/j.pocean.2016.03.004

Particle fluxes and their drivers in the Avilés submarine canyon and adjacent slope, central Cantabrian margin, Bay of Biscay

A. Rumín-Caparrós[a], A. Sànchez-Vidal[a], C. González-Pola[b], G. Lastras[a], A. Calafat[a], M. Canals[a]

[a] GRC Geociències Marines, Departament d'Estratigrafia, Paleontologia i Geociències Marines, Universitat de Barcelona, E-08028 Barcelona, Spain
[b] Instituto Español de Oceanografía, C.O. Gijón, Avda. Príncipe de Asturias 70 bis, E-33212 Gijón, Spain
* Corresponding author: miquelcanals@ub.edu

Abstract

The Avilés Canyon in the central Cantabrian margin is one of the largest submarine canyons in Europe, extending from the shelf edge at 130 m depth to 4765 m depth in the Biscay abyssal plain. In this paper we present the results of a year-round (from March 2012 to April 2013) study of particle fluxes in this canyon and the adjacent continental slope. Three mooring lines equipped with automated sequential sediment traps, high-accuracy conductivity-temperature recorders and current meters allowed measuring total mass fluxes and their major components (lithogenics, calcium carbonate, opal and organic matter) in the settling material jointly with a set of environmental parameters. The integrated analysis of the data obtained from the moorings together with remote sensing images and meteorological and hydrographical data has shed light on the sources of particles and the across- and along margin mechanisms involved in their transfer to the deep.

Our results allow interpreting the dynamics of the sedimentary particles in the study area. Two factors play a critical role: i) direct delivery of river-sourced material to the narrow continental shelf of the study area, and ii) major resuspension events caused by large waves and near bottom currents developing at the occasion of the rather frequent severe storms that are typical of the Cantabrian Sea. Wind direction and subsequent wind-driven currents largely determine the way sedimentary particles reach the canyon. While westerly winds favour the injection of sediments into the Avilés Canyon mainly by building an offshore transport in the bottom Ekman layer, easterly winds ease the offshore advection of particulate matter towards the Avilés Canyon and its adjacent western slope principally through the surface Ekman layer. Furthermore, repeated cycles of semidiurnal tides add an extra amount of energy to

the prevailing bottom currents and actively contribute to keep a permanent background of suspended particles in near-bottom waters.

High contents of lithogenics in settling particles at the three mooring stations confirm that riverine inputs are the principal source of particles to the Avilés Canyon, including the lowermost canyon, and the adjacent open slope. Primary production also has a strong influence on the amount and the composition of particulate matter, with more than 30% of the total mass flux being of biogenic origin (organic matter, opal and calcium carbonate).

1. Introduction

Submarine canyons are large seafloor geomorphological features connecting the shallower with the deeper sections of continental margins (Shepard, 1981; Nittrouer and Wright, 1994; Xu et al., 2002; Canals et al., 2006; Mulder et al., 2012). Multiple studies have demonstrated that submarine canyons act as pathways for water movements and lithogenic and biogenic materials (Gardner, 1989; Puig and Palanques, 1998; Hung et al., 2003; Palanques et al., 2006a), and are hot spots of biodiversity and biological productivity (Vetter, 1994; Vetter and Dayton, 1998; Gili et al., 1999; Vetter et al., 2010).

One of the main aims of the Spanish DOS MARES project (*Deep-water submarine canyons and slopes in the Mediterranean and Cantabrian seas: from synchrony of external forcings to living resources*) was understanding how the signal of different forcings is transferred and affects the deep ecosystem in submarine canyons and continental slopes around the Iberian Peninsula, with emphasis on the Avilés Canyon in the Cantabrian margin of the Bay of Biscay. Processes controlling particulate matter transport (e.g. atmosphere and gravitational-driven) have been studied in submarine canyons all over the world (Drake and Gorsline, 1973; Hickey et al., 1986; Durrieu de Madron, 1994; van Weering et al., 2002; Puig et al., 2004a; Paull et al., 2005; Xu et al., 2010; Pierau et al., 2011). In the Iberian Peninsula there is a strong contrast in between Atlantic margin settings and Mediterranean ones, including physiography and water depth, water mass structure and ocean dynamics.

In the Western Mediterranean Sea, east of the Iberian Peninsula, the best-studied canyons are those located in the Gulf of Lion and the Catalan margin. Some of those

canyons, especially Cap de Creus Canyon, experience high energy events in the form of seasonal dense shelf water cascading, a type of flow that erodes the shelf and slope floor and funnels large volumes of water and sediments to the deep margin and basin (Canals et al., 2006; Heussner et al., 2006). Cascading is triggered by strong, persistent, cold and dry northern winds, which cause strong heat losses and increase the density of shelf waters that eventually overflow the shelf and cascade down the slope. Coastal downwelling caused by eastern storms also enhances downcanyon sediment transport (Martín et al., 2006; Palanques et al., 2006a; Bonnin et al., 2008; Sànchez-Vidal et al., 2012). In addition of heavy precipitation and river floods carrying significant amounts of sediments and forming surface plumes along the coast, Eastern winds push surface waters against the coastline, where high waves and associated currents lead to major resuspension events of inner shelf sediments. Part of the sediment load resulting both from river floods and shelf resuspension is subsequently captured by canyons having their heads at short distance from the coastline and then is exported down-canyon (Canals et al., 2013). River floods have been identified as the main driver of down-canyon sediment transport also in submarine canyons off southern Spain, in the Alboran Sea (Palanques et al., 2005). Bottom trawling practiced on the shelf around canyon heads and along canyon flanks also triggers sediment gravity flows that move into the canyon axis, as recently shown in La Fonera Canyon, in the north Catalan margin (Puig et al., 2012).

The Atlantic continental margin west of Iberia hosts some particularly large submarine canyons according to global standards, such as Nazaré, Lisbon-Setúbal and Cascais canyons (Arzola et al., 2008; Tyler et al., 2009; Martín et al., 2011; de Stigter et al., 2011). In contrast with the tideless Western Mediterranean Sea, tidal currents there are strong enough to trigger resuspension and remobilise particulate matter (Oliveira et al., 2007), especially in upper canyon sections (de Stigter et al., 2007; 2011). The role of shelf storms, eventually combined with river floods, over particulate matter transport from the upper to the middle course of Nazaré Canyon is discussed in Martín et al. (2011). Also in the Atlantic is the northern Iberian, or Cantabrian, margin forming the southern bound of the Bay of Biscay. The Cantabrian margin is cut by several, deeply incised submarine canyons and is bounded to the east by the large, more than 2000 km long Cap Breton Canyon, where tide-initiated hydrodynamic events are able to remobilise and sustain a permanent up- and down-canyon transport of particulate matter (Mulder et al., 2012). Shelf storms also play a key role in modulating sediment transport down Cap Breton Canyon. However, in the Cap Ferret submarine canyon, in the eastern margin of the Bay of Biscay, Schmidt et al. (2014) found only a limited

downslope particle transfer from the shelf to the basin along the canyon attributed to the disconnection of this canyon from major sediment sources. Further north, in the north-eastern margin of the Bay of Biscay, in the Audierne and Blackmud canyons, particulate matter is resuspended and remobilised by strong tidal hydrodynamics (Mulder et al., 2012).

These studies support the relevance of external forcings on sediment dynamics and particle fluxes within submarine canyons and in the adjacent continental slopes. The external forcings referred to in the previous paragraphs are either atmosphere driven (wind storms, river floods, winter cooling and mixing), gravity driven (tides) or human driven (trawling induced resuspension) and all of them are capable of triggering significant sediment transport events in the submarine canyons off the Iberian Peninsula. In addition, the overall margin configuration, including the distance of canyon heads to the nearest shoreline, largely determines the capability of submarine canyons to trap coastal sediment and funnel it down course (Canals et al., 2013).

The above-mentioned background information underlines the existence of a knowledge gap on the behaviour of submarine canyons incised in the Cantabrian margin that our study contributes to fill in, as it is the first of its nature in the central Cantabrian margin. The present study focuses on sediment transfers and particle fluxes from shallow to deep, thus aiming to improve the understanding of the functioning of submarine canyons at large and of Avilés Canyon in particular, as a representative of submarine canyons in the Northeast Atlantic, so that the high productivity and biodiversity associated to these features (Vetter 1994; De Leo et al., 2010; Vetter et al., 2010) could be better understood, assessed and managed.

2. Regional setting

The Avilés Canyon is the main, 80 km long trunk of a canyon system that consists of three main branches with contrasting morphologies: the El Corbiro and La Gaviera canyons to the east and the Avilés Canyon itself to the west (Fig. 1). El Corbiro and La Gaviera merge before opening into the lowermost course of the Avilés Canyon, which opens to the Biscay abyssal plain at 4765 m depth (Lastras et al., 2012; Gómez-Ballesteros et al., 2013).

Several rivers discharge along the Cantabrian coastline. Their flows are modulated by a typical oceanic climate, with a rainy period starting in November and ending in May and a drier season taking place from June to October (Prego et al., 2008). The main contributor of freshwater and terrigenous sediment to the coastline close to Avilés Canyon head is the 138 km long Nalón River opening into the 15 km long Pravia estuary. The Nalón River is fed by a 4893 km^2 catchment area and has an annual average flow of 109 m^3 s^{-1} according to Prego et al. (2008), with annual peaks up to 1250 m^3 s^{-1}. These values made the Nalón River watershed and flow the largest in the Cantabrian river system (Prego et al., 2008). Its main tributary is the 111 km long Narcea River with a catchment area of 1135 km^2 and a mean annual discharge of 16 m^3 s^{-1} ("Confederación Hidrográfica del Cantábrico" online resources in http://chcantabrico.es/index.php/es/atencionciudadano/documentos/documentos-de-la-web/search/lang,es-es/). The Nalón River discharge to the sea is markedly seasonal in synchrony with the above-referred rainy and dry seasons. Eight main dams in the Nalón watershed, of which the tallest are Tanes in Nalón River upper course and La Barca in Narcea River, with 95 and 74 m of dam height, respectively (www.seprem.es), and a number of smaller ones, do not have an influence strong enough to wipe off the natural seasonal regime. However, the amounts of sediment trapped behind those dams remain non-quantified. Of the twenty-eight Cantabrian rivers investigated by Prego et al. (2008), the Nalón River is the one with the highest load (836 m^3 s^{-1}) of total suspended solids (TSS) and is identified as the most important Cantabrian river in terms of TSS contribution to the Bay of Biscay with 379.900 t y^{-1} representing 33% of the total.

Consequently with its geographical location, the water column structure of the Bay of Biscay, and the Cantabrian Sea in particular, corresponds to the Northeast Atlantic one (Lavín et al., 2006). Namely: (1) surface waters extending down to the winter maximum depth (~250 m) of the mixed layer (González-Pola et al., 2007), which are characterized by a pronounced inter-annual variability linked to seasonal cycles; (2) the East North Atlantic Central Water (ENACW) from the base of the mixed layer down to 400-600 m; (3) the Mediterranean Outflow Water (MOW) that is located below the ENACW and extends down to depths of 500 to 1500 m (Iorga and Lozier, 1999a); and (4) the Bottom Water (BW) extending down to the seafloor as a deep water mass formed after the mixing of several water masses including the North Atlantic Deep Water (NADW), the Lowered Deep Water (LDW) and Antarctic Bottom Water (ABW) (Botas et al., 1989; Pingree and Le Cann, 1992; van Aken, 2000a).

The ENACW results from winter mixing over the area surrounded by the North Atlantic Current (NAC) and the Azores Current (AC) (Pollard and Pu, 1985; Pollard et al., 1996). Two varieties of ENACW are defined according to their origin, temperature and salinity (Ríos et al., 1992). The denser variety, or subpolar mode of the ENACW, forms in the southern border of the NAC. In the Bay of Biscay it flows weakly and experiences an anticyclonic recirculation (Pingree, 1993). The lighter variety, or subtropical mode of the ENACW, forms at the northern boundary of the AC and is conveyed along the northwestern and north Iberian upper continental slope by the Iberian Poleward Current (IPC) (Haynes and Barton, 1990). The IPC circulates poleward along the western and northern Iberian continental shelf and slope, eventually reaching the French Armorican shelf (Pingree and Le Cann, 1990). The MOW results from the discharge of Mediterranean dense deep water into the Atlantic Ocean through the Gibraltar Strait. The northern branch of the MOW flows along the Western Iberian margin as a slope current (Iorga and Lozier, 1999a, 1999b; van Aken, 2000b) and reaches the Bay of Biscay with speeds between 2 and 3 cm s^{-1} (Pingree and Le Cann, 1990; Díaz del Río et al., 1998). The BW draws a cyclonic recirculation cell over the Biscay abyssal plain with a poleward current velocity of 1.2 cm s^{-1} nearby the foot of the continental margin (Dickson et al., 1985; Paillet and Mercier, 1997).

Seasonal wind patterns have a significant impact on the sea surface circulation over the shelf and slope of the study area (Charria et al., 2013). NNE to easterly winds, which usually are more common from April to September, trigger a westward shelf and slope surface circulation and promote coastal upwelling. The presence of the Avilés Canyon system seems to enhance upwelling during such situations, which results in an up-canyon flow (Ruiz-Villareal et al., 2004). In contrast, NW winds, which can be very strong and usually are dominant from October to March, lead to an eastward shelf and slope surface circulation and coastal downwelling. Under these conditions, the submarine canyon does not seem to have any effect on the incident slope current (Ruiz-Villareal et al., 2004). The influence of the IPC surface flow over the western Iberian and Cantabrian slopes in winter extends to the first 200-300m depth so impacting the upper slope (Frouin et al., 1990; Haynes and Barton, 1990; Pingree and Le Cann 1990; Pingree and Le Cann 1992; Serpette et al., 2006; Friocourt et al., 2007; Le Cann and Sarpette, 2009).

Semi-diurnal tidal oscillations on the Avilés shelf are highly energetic and can dominate current dynamics (Fanjul et al., 1997). Indeed, barotropic tides above steep topographies, such as submarine canyons, give rise to internal tides, especially where

the slope gradient becomes critical (i.e. wherever the topographic slope matches the propagation angle of the internal tide beams) (Baines, 1982; Cacchione et al., 2002). According to data from "Puertos del Estado", the mean meso-tidal range at the coast close to Avilés Canyon for the period 1996-2013 ranged between 1.95 m and 4.68 m at neap and spring tides, respectively, and exceeded 5 m during equinoctial tides. In the Bay of Biscay, the dominance of the semi-diurnal barotropic forcing over the shelf-break and slope makes the internal tide to be markedly semi-diurnal (Pingree and New, 1989). The capability of such tides to influence sedimentary processes by triggering bottom currents fast enough to resuspend sediment has been described in the nearby Aquitanian margin of the Bay of Biscay (Durrieu de Madron et al., 1999).

3. Materials and methods

3.1 Forcing conditions

Wind speed and direction at 3 m above the sea surface and wave height and direction were obtained from Cabo Peñas Seawatch buoy measuring waves as well as atmospheric and oceanographic parameters at an hourly frequency (Álvarez-Fanjul et al., 2003). The buoy, which belongs to the Deep Water Network from "Puertos del Estado", is moored at 615 m of water depth on a sort of plateau in the western flank of the Avilés Canyon upper course (Fig. 1). Near surface currents are not corrected for platform motion and all the data gathered by the network buoys is subject to a quality control procedure to find inconsistencies and other anomalies in the datasets.

The buoy data have been crosschecked by linear correlation (not shown) with the coded WANA point 1053075 (see location in Fig. 1) in order to further validate the wind and wave data used in our work. The WANA network delivers hourly averaged time series of wind (at 10 m above the sea surface) and wave parameters obtained from a reanalysis product performed by "Puertos del Estado" in collaboration with "Agencia Estatal de Meteorología".

The wind-drag-induced Ekman transport perpendicular to the coastline (Q_y) is normally taken as an Upwelling Index (UI). This index is an estimate of across-slope transport depending on local wind. In our study, the dominant orientation of the coastline is in the east-west direction and the UI magnitude expresses volume of water transported in the

north-south direction by lineal km of shore (in m^3 s^{-1} km^{-1}). UI has been calculated from Cabo Peñas buoy wind data according to Bakun (1973) using equation

$$UI = Q_y = -\frac{\tau_x}{f \cdot \rho_w}, \qquad [1]$$

where τ_x is the wind stress for the *x* component, f is the Coriolis parameter calculated as $f = 2\Omega \sin \Phi$ at 43° of latitude, and ρ_w is seawater density (1025 kg m^{-3}). Upwelling is characterized by positive values of Q_y whereas negative values are indicative of water masses piling up towards the coast (i.e. downwelling). The wind stress for the *x* component is calculated with equation

$$\tau_x = \rho_a \cdot C_d \cdot \sqrt{U^2 + V^2} \cdot U, \qquad [2]$$

where ρ_a is the density of air, U and V are the eastward and northward wind components, respectively, and C_d is the neutral drag air coefficient computed following Smith (1988).

Discharges by Nalón River and its main tributary, the Narcea River, measured from gauging stations located at 23 and 22 km from the river mouth, respectively, have been obtained from EDP group of companies.

Estimates of Chl-a concentrations are from the Giovanni online data system, developed and maintained by the NASA Goddard Earth Sciences (GES) Data and Information Services Center (DISC), using as source the Moderate Resolution Imaging Spectroradiometer (MODIS). Data have been gridded from 43.4ºN to 45ºN, and from 7.5ºW to 4ºW in order to include the mooring locations and the areas adjacent to Avilés Canyon. Net primary production data were downloaded from the Ocean Productivity website (http://www.science.oregonstate.edu/ocean.productivity/) and calculated using the Vertically Generalized Production Model (VGPM) (Behrenfeld and Falkowski, 1997). For VGPM, net primary production is a function of chlorophyll, available light, and the photosynthetic efficiency.

Forcing conditions have been also considered indirectly by means of a two-way statistical ANOVA analysis intended to examine the factors responsible for the variability of Total Mass Fluxes (TMFs) in the Avilés Canyon and in its western slope.

For this analysis, two fixed factors were considered: month of collection and trap depth (Table 2; see section 4.3).

Checking to what extent external forcings are correlated to the temporal variability of TMFs has been carried out by means of a cross-correlation analysis (Table 3; see section 4.3). Given that raw time series with different time steps ranging from hourly to daily periods present occasional gaps, data were transformed into regular and continuous time series prior to the statistical analysis. All data were re-sampled to a time step equivalent to the sampling period of the sediment traps and such time lapse has been used as a "lag" to evaluate time-lagged correlations between time series. Gaps in TMFs in AC2000T trap were linearly interpolated considering the low variability of TMFs in the other sediment traps during the data gap (Fig. 4).

3.2 Multibeam data acquisition

Prior to the deployment of the mooring lines, and in order to accurately identify the more convenient locations to install them, a seabed high-resolution bathymetric survey including the acoustic characterization of the seabed of the Avilés Canyon and the adjacent continental slope was performed. Multibeam data covering 5682 km^2 of the Cantabrian margin around the Avilés Canyon was acquired in October-November 2011 during the COCAN cruise onboard R/V "Miguel Oliver". Data were obtained with a Simrad EM302D multibeam echo-sounder operated in equidistant mode with swath widths between 600 m on the shelf and 6000 m on the abyssal plain. The complete dataset was processed onboard using Caris HIPS and SIPS software, resulting in a general 20 m-grid-size digital terrain model.

3.3 Experimental design

The high-resolution multibeam bathymetry maps evidenced the complex morphology of the Avilés Canyon system and the adjacent continental slope. Jointly with backscatter imagery (not shown), multibeam bathymetry served as background information to decide where to deploy the mooring lines to investigate the across margin transport of particulate matter and characterise the associated ambience conditions, both within and outside the Avilés Canyon. Two moorings (AC2000 and AC4700) where placed in the middle course and lowermost course of the canyon at 2000 m and 4700 m depth, respectively (Fig. 1 and Table 1). AC2000 was deployed in order to capture sediment fluxes eventually arriving both from the shelf-incising set of tributaries known as La

Vallina branches and from the Avilés Canyon head and upper course (see section 4.1). AC4700 was deployed in a very flat area where the Avilés Canyon widens significantly and opens into the Biscay abyssal plain down course of La Gaviera Canyon mouth which main tributary is El Corbiro Canyon (Fig. 1). Therefore, AC4700 offered a good potential to capture sediment fluxes eventually arriving from the entire Avilés Canyon system. A third mooring (WS1200) was deployed as a control station at 1200 m depth in the open slope west of Avilés Canyon (Fig. 1).

All mooring lines were equipped with automated sequential sediment traps, high-accuracy conductivity-temperature recorders and current meters. They were deployed during one complete annual cycle in two consecutive periods, from March 2012 to September 2012 and from September 2012 to March 2013.

The AC2000 mooring line was equipped with two Aquadopp current meters at 44 and 820 m above the bottom (mab), and two PPS3 sediment traps coupled with SBE37 recorders at 46 m and 822 mab. Hereafter, AC2000T and AC2000B will be used to refer to the mid-water (at 820 mab or 1200 m of water depth) and near-bottom levels in this mooring, respectively. The AC4700 mooring line was equipped with a single RCM8 current meter at 44 mab and a PPS3 sediment trap at 46 mab. The WS1200 mooring line was equipped with a pair of current meters, which were an Aquadopp acoustic Doppler current meter at 160 mab and an Aanderaa RCM8 rotor current meter at 44 mab, and a Technicap PPS3 sediment trap coupled with a SBE37 high-accuracy conductivity-temperature recorder at 46 mab.

The PPS3 Technicap sequential sediment traps have a 0.125 m^2 collecting surface and a 2.5 height/diameter ratio in its cylindrical part. They are equipped with 12 receiving cups (Heussner et al., 1990), which were filled with a buffered 5% (v/v) formaldehyde solution in 0.45 µm filtered seawater. This solution is used to prevent the degradation of the collected particles in the retrieving cups and also to avoid fragmentation and degradation of swimmers occasionally entering the sampling cups. All traps collected settling particles synchronously and uninterruptedly with a sampling interval of 15-16 days during the first and second deployment periods except the last three collecting bottles of February 2013, which remained opened 7 days in order to adjust the total sampling interval to the scheduled recovery dates. Traps worked properly from 16 March 2012 to 23 September 2012, and from 1 October 2012 to 8 March 2013, except AC2000T, which stopped collecting samples before the end of the first deployment period, on the first of August 2012.

10

Aandera and Aquadopp current meters were set with sampling intervals of 15 minutes at upper levels and 30 minutes near the bottom. A technical failure of the current meter deployed at AC4700 resulted in the complete data loss at this water depth.

3.4 Trap collection efficiency

Trap collection efficiency has been checked by examining the pitch and roll sensors of the current meters. Efficiency can be compromised by trap tilting (Gardner, 1985) and also because of the potential of perturbation of trap mouths on lateral flows causing biases in the collection of sinking particles (e.g. Baker et al., 1988; Gardner et al., 1997; Buesseler et al., 2007 and references therein).

Data from the current meter pressure sensors show that sediment trap tilting never exceeded 11°, even during current speeds as high as 40 cm s^{-1}. According to Gardner (1985) TMFs would not have been affected (see explanation on how TMFs have been calculated in section 3.5). Our results compare well with those obtained by Bonnin et al. (2008) in their collecting efficiency experiment using the same PPS3 Technicap sediment traps. These authors concluded that their mooring lines were maintained taut, close to vertical, never tilting more than 15°, during strong current episodes (up to 82 cm s^{-1}).

Since we do not have enough information to detect any effect of perturbation by trap mouths on lateral flows, and in order to be consistent with the extensive published data using the same sediment traps in other locations around the Iberian Peninsula and beyond (e.g. Heussner et al., 1999; Fabrés et al., 2002; Miquel et al., 2011; Stabholz et al., 2013), we assume that hydrodynamics over the trap mouth did not bias mass fluxes.

3.5 Sediment trap sample processing and analytical methods

After recovery, samples were stored in the dark at 4ºC until they were processed following a modified version of the methodology of Heussner et al. (1990). Swimming organisms were removed in two steps according to its size: large swimmers were removed by wet sieving through a 1 mm nylon mesh and organisms of less than 1 mm were handpicked using fine tweezers under a microscope. A high-precision peristaltic pump robot was used to split samples into aliquots through repeated division of the

sample. Samples were then repeatedly rinsed with Milli-Q water and centrifuged to remove formaldehyde and salt, and freeze-dried before chemical analyses. The dried fraction was weighted to obtain the total mass. TMFs were calculated as follows:

$$TMF\ (g\ m^{-2}\ d^{-1}) = \frac{Sample\ dry\ weight\ (g)}{Collecting\ area\ (m^2) \cdot Sampling\ interval\ (days)} \qquad [4]$$

Total carbon, organic carbon (OC) and nitrogen (N) contents were analysed at "Centres Científics i Tecnològics" of Universitat de Barcelona using an elemental analyser Thermo EA Flash 1112. In order to determine the OC content, samples were first decarbonated with 25% HCl adding repeatedly aliquots of 100 µL until no effervescence was observed. Between each acidification, samples were dried during 8 h at 60ºC. Organic matter (OM) content was calculated as twice the organic carbon content. Inorganic carbon content was calculated as total carbon minus organic carbon. Carbonate content was calculated assuming that all inorganic carbon is contained within calcium carbonate (CaCO$_3$), using the molecular mass ratio of 100/12.

Biogenic silica was analysed by extracting the amorphous silica by means of a two-step 2.5 h extraction with 0.5M Na$_2$CO$_3$ separated by centrifugation of the leachates according to Fabrés et al. (2002). Si and Al contents of leachates were analysed with Inductive Coupled Plasma Atomic Emission Spectrometer (ICP-AES). The Si content of the first leachate was corrected by the Si/Al ratio of the second one, and corrected biogenic Si concentrations were transformed to opal by multiplying by a factor of 2.4 (Mortlock and Froelich, 1989).

Abundance of the lithogenic fraction was obtained by subtracting from the total mass the part corresponding to major biogenic components, assuming that the amount of lithogenics (%) was = 100 - (%OM + %CaCO$_3$ + %opal).

3.6 Calculation of lateral fluxes of suspended sediment

Advection of suspended matter in Avilés Canyon and in the slope west to the canyon has been calculated from data acquired by the current meters and turbidity meters deployed near the bottom. Recorded Nephelometric Turbidity Units (NTU) have been converted to suspended sediment concentration (SSC) using equation [3] by Guillén et al. (2000):

$$SSC \ (g \ m^{-3}) = 1.74 \cdot Turbidity \ (NTU) - 1.32 \qquad\qquad [3]$$

SSC has been multiplied by current speed to obtain the magnitude (in g m^{-2} s^{-1}) of lateral fluxes (LF).

4. Results

4.1 Morphology of the Avilés Canyon

The Avilés Canyon is incised about 25 km in the central Cantabrian continental shelf, which is 45 km wide west of the canyon but only 13 km wide ahead of the canyon tip located 18 km WNW of the large coastal promontory of Cabo Peñas (Fig. 1). The tip of the canyon is at 130 m of water depth and opens to a canyon head and upper course that display three sharp bends probably related to underlying tectonic lineations (Lastras et al., 2012). Several tributaries join the Avilés Canyon upper and middle course, mostly through its western flank at axial depths ranging between 1300 and 2100 m (Fig. 1). The group named La Vallina branches includes four main tributaries, which are SW-NE oriented and also markedly incised on the shelf (Fig. 2a-c). Except the westernmost one, La Vallina branches are straight or nearly straight. The two eastern branches show smoothened right flanks along the length incised in the continental shelf, which oppose to gullied left flanks (Fig. 2 b, c). In the two western branches, the two flanks look moderately smoothened with some gullies occurring locally. The lower Avilés Canyon is SSW-NNE oriented and its increasingly wide floor is interrupted by a series of overdeepenings (Lastras et al., 2012). The Avilés Canyon mouth opens to the Biscay abyssal plain in an area occupied by a faint sedimentary wave field (Gómez-Ballesteros et al., 2013).

4.2 External forcings

Nalón River discharge time series show increased values in early February 2012 (up to 1071 m^3 s^{-1}), mid April 2012 (602 m^3 s^{-1}), late January 2013 (853 m^3 s^{-1}), and late March 2013 (669 m^3 s^{-1}). Other less marked increases occurred in November and December 2012 (up to 300 m^3 s^{-1}) and February-March 2013 (up to 484 m^3 s^{-1}) (Fig. 3a).

Chl-a higher concentrations in March 2012 and April 2013 (Fig. 3b) correspond to the well-known seasonal phytoplankton spring bloom in the region (e.g. Fernández and Bode, 1991).

The wind regime during the entire monitoring period from March 2012 to March 2013 is characterized by a recurrent alternation between easterly and westerly winds as a response to the coastal polarization of winds (Fig. 3c). Higher wind speeds were recorded during westerly wind bursts (Fig. 3c, d). However, there were also several periods of strong winds with an important meridional component (such as December 2012, Fig. 3c, d). Wave direction (i.e. the direction from which waves arrive to the study area in degrees counted clockwise from the geographical North) shows a marked northwest component during the studied period (Fig. 3e). Maximum significant wave heights (Hs) were recorded in mid April 2012 and during late January-early February 2013 (Fig. 3f) under predominant westerly winds.

4.3 Spatial distribution and variability of mass fluxes

The time series of vertical TMFs recorded in the sediment traps deployed in the Avilés Canyon and on the nearby open slope are shown in Figure 4. TMFs fluctuate at least one order of magnitude within all stations.

At the WS1200 (near-bottom) open slope station west of Avilés Canyon, TMFs reached a maximum of 11.94 g m^{-2} d^{-1} in March 2012, whereas during the rest of the experiment, values remained below 1 g m^{-2} d^{-1}, with a minor increase in autumn 2012 (Fig. 4a).

In the Avilés Canyon middle course AC2000 station, TMFs increase with increasing trap depth. At the near-bottom level (AC2000B), higher fluxes occurred during the middle-end of winter and in spring (15.65 g m^{-2} d^{-1} in April 2012, which represents the top value of TMFs recorded in all stations, and up to 5.24 g m^{-2} d^{-1} in February 2013). Relatively low fluxes were recorded during the rest of the year (between 0.19 and 2.12 g m^{-2} d^{-1}) (Fig. 4b), although a continuous TMF increasing trend took place from October 2012 until almost the end of the experiment. In contrast, in the upper level (AC2000T), TMFs varied from a maximum of 2.57 g m^{-2} d^{-1} in April 2012 to a relative minimum of 0.047 g m^{-2} d^{-1} in July 2012. In October 2012 TMFs increased again till reaching a second relative maximum of 0.74 g m^{-2} d^{-1} in November and December 2012. From December 2012 to the end of the experiment, TMFs decreased

14

progressively to 0.046 g m^{-2} d^{-1} recorded in February 2013 (Fig. 4b). In comparison with the deeper AC2000B trap, variability in TMFs at the shallower AC2000T is much smaller.

Compared to all other stations and levels, TMFs at the near-bottom AC4700 canyon lowermost course station are much lower, usually around or below 0.35 g m^{-2} d^{-1}, except for two peaks of up to 0.94 and 1.86 g m^{-2} d^{-1} recorded in May 2012 and March 2013, respectively (Fig. 4c).

The ANOVA analysis shows that the interaction between the month of collection and the trap depth are the main source of variance in the studied area (31%). The month of collection by itself also is significant, representing 21% of the overall variability, which by extension suggests that the variability in TMFs mostly relates to the seasonality of the external forcings. Therefore, these two variables account for 52% of TMFs variability. However, 40% of the variability remains unexplained (residual) (Table 2).

As shown in Table 3, the highest correlation coefficient (>0.7) between time series of external forcings and TMFs corresponds to wave height and wind speed at time lag 1 (15 days) for the mid-water (~1200 m of water depth) trap AC2000T. Good correlation coefficients (~0.6) are also found for these two variables again at time lag 1 for the near-bottom (1954 m of water depth) trap AC2000B. There is a good correlation (~0.7) for the same middle canyon station AC2000 at both levels, mid-water and near-bottom, with total river discharge at time lag 3 (45 days). At the near-bottom, western open slope trap WS1200 the correlation of TMFs and the three variables considered in Table 3 is weaker (~0.4-0.5) and occurs at time lag 2 (30 days) for wave height and wind speed and at time lag 4 (60 days) for total river discharge. Except for wind speed, high cross-correlation coefficients between AC4700 and the external forcings in Table 3 have been found at negative time lags, which are non-representative and therefore will not be considered in the discussion.

LFs are markedly different in the near-bottom stations WS1200 and AC2000B (Fig. 4d, e). In the open slope station WS1200, LFs show a background level close or slightly above 0.05 g m^{-2} s^{-1} and below 0.1 g m^{-2} s^{-1} during most of the time, with some spikes from June to September 2012 and in January 2013. The most prominent of them occurred in July 2012 reaching 3 g m^{-2} s^{-1} (Fig. 4d). It was also in January 2013 when peak LFs (up to 2 g m^{-2} s^{-1}) were recorded in station AC2000B, where a few minor

spikes are also visible (e.g. at the end of April 2012 and in the first half of August 2012, both with 0.6 g m^{-2} s^{-1}) above a similar background level than in WS1200 (Fig. 4e).

4.4 Mean composition of particle fluxes and changes through time

Lithogenics clearly dominate settling particles at all stations, with averaged annual values between 53.05% and 66.98%, and fluxes around 0.17 and 1.37 g m^{-2} d^{-1} (Table 1). The temporal variability of the lithogenic content is quite similar among all stations but AC2000B (Fig. 5a), with higher values during autumn and winter (i.e. from September 2012 to February 2013) and lower values during spring and summer (i.e. from March 2012 to August 2012). AC2000B shows the highest averaged annual value and also the lowest range of interannual variation (i.e. from 62.42% to 74.11%) (Fig. 5a and Table 1). The lithogenic contribution to TMFs never is less than 37% (Fig. 5a). On average it is almost six percentage points lower in AC2000T (mid-water) than in AC2000B (near-bottom), and fourteen percentage points lower in AC4700 (near-bottom) than in AC2000B. This data evidences a decrease in the percentage of lithogenics with, first, increasing distance to the seafloor and, second, increasing canyon depth.

Averaged annual CaCO$_3$ fluxes are lower than lithogenics, ranging between 0.12 and 0.47 g m^{-2} d^{-1} (Table 1). Besides, CaCO$_3$ relative contents display a trend opposite to the lithogenics one, with lower percentage values during autumn and winter (i.e. from September 2012 to February 2013) and slightly higher values during spring and summer (i.e. from March to August 2012) (Fig. 5b). Higher variations were recorded during spring especially at the lowermost canyon and open western slope, where the CaCO$_3$ averaged annual percentage is the highest among all traps. Like for the lithogenics, AC2000B shows the lowest range of interannual variation (i.e. from 17.16% to 30.7%), in parallel with the lowest averaged annual value, close to the one of AC2000T, with 24.42% and 24.93%, respectively (Fig. 5b and Table 1). For the two near-bottom traps deployed inside the canyon, the CaCO$_3$ annual mean content increases with water depth, being about ten percentage points higher at the lowermost canyon (AC4700) than in the middle canyon (AC2000B) (Table 1). It is noteworthy that during the second half of the studied period, CaCO$_3$ records in all traps present a rather similar evolution.

OM fluxes are relatively low, with averaged annual values ranging from 0.025 to 0.14 g m^{-2} d^{-1} and averaged percentages around 8-10% (Table 1). The atomic N to OC ratio

(N:OC), which is widely used to examine OM sources and source shifts in settling particles, is on average ~0.11 for all traps (Figure 5c). Time series show enhanced N:OC ratios (0.12-0.16) and OM relative abundance (16-18%) at station WS1200 in May 2012 and March 2013, thus indicating a marked spring seasonal signal on settling particles at this station. Similar variations were recorded at the upper trap AC2000T of station AC2000 (Fig. 5c), which also displays the highest annual OM contents (Table 1). Both traps, WS1200 and AC2000T, are in the 1150-1200 m depth range below the sea surface (Table 1). In contrast, settling particles at the near-bottom traps AC2000B and AC4700 within the canyon show rather stable N:OC ratios and OM relative abundances (around 0.8-0.13 and 6.5-8.6%, respectively), with only minor fluctuations except for a peak recorded at AC4700 in June 2012 (reaching 12%). By the end of the time series OM contents at all traps and stations reached minimum values to start increasing again till the end of the sampling period in March 2013. This increase was particularly important at WS1200 and AC2000T (Fig. 5c). The parallelism of the OM records for these two traps is noticeable and, except for the above-mentioned final part of the time series, they do not seem to be correlated with the near-bottom traps AC2000B and AC4700 (Fig. 5c).

Averaged annual opal fluxes range between 0.017 and 0.09 g m^{-2} d^{-1} (Table 1) and opal relative abundance shows different patterns depending on mooring location and water depth (Fig. 5d). At the two traps in the same depth range below the sea surface, the western open slope WS1200 (near-bottom) and the AC2000T (mid-water) over the middle canyon, opal content shows an obvious temporal variability peaking up at 12% in March 2012 and March 2013. In the other two, in-canyon, near-bottom traps AC2000B and AC4700, opal contents do not show a clear seasonal signal and the fluctuation rate is much less, especially for AC2000B (Fig. 5c). Similarly to OM, enhanced opal relative abundances were recorded by the end of the observational period at all stations, weakly at AC2000B and strongly at WS1200 and AC2000T. Contribution of opal relative abundance to the total mass does not represent more than 15% at any trap, and opal mean annual content remains in the range from 2.20% to 4.36 %, with the lowest and highest values corresponding to the near-bottom canyon traps AC2000B and AC4700, respectively. WS1200 and AC2000T display very similar values (3 and 3.09%).

5. Discussion

5.1 Particle sources and dispersal patterns

Our results show the dominance of river-sourced lithogenics in sinking particles in the study area. Quartz, feldspars, heavy minerals and aluminosilicates mainly constitute these particles. The dispersion of riverine water and lithogenic particles in the vicinity of the Avilés submarine canyon appears to be affected by seasonal reversals of sea surface circulation. During autumn and winter, prevailing westerly winds induce an eastward shelf-slope circulation associated to downwelling conditions, which pushes sediment-loaded river plumes away from Avilés Canyon to the east, towards Cabo Peñas and beyond, as shown in the MODIS image of 21 January 2013 (Fig. 6a). Eastward surface currents associated with an onshore surface Ekman transport may also lead to a coastal confinement of river plumes, as also shown in Figure 6a. Below the surface layer where Ekman transport occurs, there must be a compensatory circulation, directed in opposite sense. Downwelling conditions due to westerly wind forcing will then lead to an eastward shelf current that (if interacting with the bottom, which is generally the case under winter high energy conditions) corresponds to offshore transport in the bottom Ekman layer. This is because in a bottom Ekman layer the Ekman transport is directed to the right of the bottom stress, in the same way that in a surface Ekman layer the Ekman transport is directed $90°$ to the right of the wind stress in the Northern Hemisphere. However, given that the stress at the seafloor is in the opposite direction of the prevailing current, the bottom Ekman transport is $90°$ to the left of the surface current, with the Ekman spiral turning counterclockwise with increasing depth in the Northern Hemisphere (Taylor and Sarkar, 2008).

Westerly wind pulses also reinforce the entrance of the eastward-flowing poleward slope currents over the Cantabrian margin (e.g. González-Pola et al 2005), which extend from the surface to about 250-400 m depth (Pingree and Le Cann, 1990; Gil and Gomis, 2008). Contrarily, during spring and summer, when easterly winds prevail, the shelf circulation is mainly westwards (Charria et al., 2013). Westward surface currents are associated with an upwelling component able to entrain river plumes and resuspended shelf sediments towards the shelf edge, as shown in the MODIS image of 4 May 2013 (Fig. 6b), taken after an enhancement in the discharge of Nalón River (Fig. 3a). The same wind forcing then builds a westward coastal jet, which in the bottom Ekman layer originates onshore bottom transport favouring the retention of

18

resuspended sediments over the shelf. Indeed, in the nearby continental shelf of the Basque country to the east, Jouanneau et al. (2008) reported that prevailing winds and surface currents also redistribute preferentially suspended sediment river plumes, with particle settling occurring in periods of calm.

The relation of increases in river discharge (Fig. 3a) and TMFs in the Avilés Canyon and the western open slope (Fig. 4a, b) is an interesting point of discussion. Our dataset seems to suggest a connection in between sustained high river discharge conditions from January to February 2013 and the increases of TMFs in near-bottom traps AC2000B and, perhaps, though delayed, AC4700 (Fig 4a-c). However, this connection is not apparent neither for AC2000T and WS1200 nor for other shorter events of enhanced river discharge, such as the one in April 2012, which had apparently no effect on TMFs in the shallower stations, as shown by high TMFs occurring before the discharge peak (Figs 3a and 4 a, b). The relation of the sharp discharge peak of February 2012 (Fig. 4a) with TMF peaks in early 2012 is also unclear, as the TMF tallest peak appears in March in WS1200, which is farther from Pravia estuary, and in April in the closer AC2000 at both levels, although with markedly different intensities (Fig. 4a, b). The March 2012 prominent peak in WS1200 is synchronous with a major chlorophyll-a peak under the dominance of easterly winds and resulting westward circulation. However, river discharge, wind speed, wave height and current speed were low during that time (Fig. 4). The composition of mass fluxes at WS1200 in March 2012 (Fig. 5) points to a phytoplankton signal overimposed on the generally dominant lithogenic component (see section 4.4).

Without totally precluding some direct connection between the river and the submarine canyon under specific conditions, it is worth considering other dispersion mechanisms that may act either by themselves or in combination with a more direct connection and amongst themselves. The normal winter mixed layer in the region hardly exceeds the depth of the shelf-break, as it is about 250 m thick only (González-Pola et al., 2007). Therefore, a direct influence of winter convective mixing events on sedimentary particle dynamics at depths where the moorings were deployed should not be expected and, at the most, can only be indirect and likely minor. Only exceptionally the mixed layer reaches larger depths (e.g. in 2005; Somavilla et al., 2009), thus increasing the options to directly imprint sedimentary processes in the canyon. During winters 2012 and 2013 atmospheric forcings were not exceptionally strong and the mixed layer did not reach unusual depths (R. Somavilla, personal communication). Below the maximum winter mixed layer, the density gradient characteristic of the local permanent pycnocline (van

19

Aken, 2001) may hinder the vertical transport of particulate matter, especially of the lighter fractions. In this context, processes favouring lateral advection of sediments from the shelf become good candidates for triggering major arrivals of river-sourced particles into the canyon. Our hypothesis is that river-sourced particles temporarily accumulate on the shelf till high-energy forcing conditions (see section 5.2) able to resuspend and lead to bottom Ekman layer transport carry them into the canyon. This involves critically assessing the bottom transport against the surface transport to avoid misleading interpretations (see section 5.2.1). A similar mechanism of delayed transfer to the continental slope and submarine canyons has been described in other margin settings, such as the Gulf of Lion and the North Catalan margin, where dense shelf water cascading and eastern storms provide such high-energy conditions (Canals et al., 2006; Ulses et al., 2008a; Sànchez-Vidal et al., 2012).

Marine primary production is the second main source of sinking particles in the study area. In the shelf and offshore waters of the Cantabrian margin there is a seasonal succession of phytoplankton species that relates directly to the hydrographical variability (Fernández and Bode, 1994). In winter and spring, intense vertical mixing leads to a homogenized, nutrient-rich water column and noticeable diatom-dominated phytoplanktonic blooms (Fernández and Bode, 1994), as shown in March-April 2012 and April-May 2013 (Figs. 3b, 7). In contrast, in summer and autumn, reduced vertical mixing accompanied by enhanced solar heating leads to a nutrient-depleted stratified upper layer and low primary production. Under these conditions, dinoflagellates, which are able to migrate towards nutrient-rich layers, dominate the phytoplanktonic community (Fernández and Bode, 1994). Occasionally, upwelling alters the above-described hydrographic pattern by reinforcing vertical mixing, injecting extra inputs of inorganic nutrients to the surficial layers and increasing primary production (González-Quirós et al., 2003). Upwelling events can be traced as intermittent cold-water tongues close to the coast, often nearby Cabo Peñas promontory, where topographic effects enhance this process (Botas et al., 1989). During the studied period, the spring primary production bloom in 2012 occurred mostly offshore in the central part of the Bay of Biscay, while in 2013 the bloom maximum was observed closer to the Cantabrian coast (Fig. 7). More persistent upwelling favourable conditions in 2013 than in 2012, especially from mid March to late April (Fig. 8), likely led to a higher supply of new nutrients close to the shoreline along the entire Cantabrian margin, thus resulting in a pronounced coast-parallel phytoplankton bloom (Fig. 7). A stronger and more constant river discharge during 2013 (Fig. 3a), also contributing new nutrients to the coastal area, could have enhanced the coast-parallel primary production too. It should be

noted, however, that the algorithms used to estimate primary production are susceptible to interference caused by the complex optical properties of the constituents commonly found in coastal waters, where the influence of river outflows, riverine suspended sediments and dissolved OM may confuse the interpretation of satellite-based ocean colour data (Moreno-Madriñán and Fischer, 2013). Further elaboration on this aspect is hampered by the closure of the last collecting cup before the 2013 phytoplanktonic bloom.

The composition of settling particles allows defining two particle settling regimes. First, the record of the shallower sediment traps both on the open slope (WS1200, near-bottom) and the canyon middle course (AC2000T, mid-water) was markedly seasonal and showed relatively high contents of OM and opal, which most likely resulted from pelagic settling of biogenic particles. Second, the record of the near-bottom traps at the canyon middle and lowermost course AC2000B and AC4700 did not show any evidence of seasonality because of the dilution of biogenic components amidst more abundant, laterally advected lithogenic material. In the shallower environment including the mid-water AC2000T and the near-bottom WS1200 sediment traps, relatively high opal abundance (>12%) found in March 2012 (Fig. 5d) can be directly related to the pelagic settling of material derived from blooms dominated by oceanic tychoplanktonic diatoms and chrysophyceans with siliceous skeletons and/or cysts. It is noteworthy that in April 2012, 16 to 30 days after the opal peak at AC2000T, an increase is observed at AC2000B too (Fig. 5d). This suggests that particles settling at 1200 m of water depth most probably reached the seafloor. The 800 m of depth difference between AC2000T and AC2000B, and the 30 days of delay result in a siliceous skeletons and/or cysts sinking speed of about 26 m d^{-1}, which is within the range published by Asper (1987) for sinking diatom aggregates.

Following the opal peak in March 2012, an increase in OM relative abundance was also detected in May 2012 in the shallower WS1200 (near-bottom) and AC2000T (mid-water) traps. Such a peak following that in opal relative abundance can be explained by a growth response of consumers (zooplankton) after an increase in phytoplankton, which is in agreement with Stenseth et al. (2006). During this period, in the same two traps N:OC ratios were slightly higher than during most of the following fall and winter months, which according to the high N content of marine OM (N:OC >0.12), might be a direct signal of the arrival of OM from marine algae. Slightly higher OM relative abundances were recorded from October to December 2012 at both WS1200 and AC2000T, which might be connected to an autumn phytoplankton bloom that may

occur in the region during the transitional stage from stratification to mixing (Fernández and Bode, 1991). In September 2012, prevailing easterly winds and accompanying westward surface currents (Fig. 3c, g) led to a prolonged upwelling-favourable situation. This situation, jointly with some short-lived easterly wind episodes in October and November, might have favoured the nutrient replenishment of the surface layer and thus, phytoplankton growth. Bottom-up processes, driven ultimately by meteorological and hydrodynamic forcings, have been widely recognized as key factors in modulating phytoplankton growth and population dynamics (Margalef, 1978).

About the similarities in the evolution of OM relative contents of WS1200 (near-bottom) and AC2000T (mid-water), located at about the same depth (1150-1200 m) below the surface (see section 4.4), it must be pointed out that both traps lie within the background flow of the slope currents (e.g. Pingree and Le Cann, 1990), which may help homogenizing OM relative contents because of along slope transport. The persistently high relative abundance of lithogenics in the near-bottom AC2000B trap (Fig. 5a) suggests a dilution effect of OM and opal biogenic particles. Higher opal relative abundance in the near-bottom lowermost canyon course trap (AC4700) than in AC2000B and, for most of the time, the shallower traps (Fig. 5d), suggests a distinct behaviour of the lower canyon course, that seems to be more influenced by pelagic settling and less by advective transport from the inner continental margin. OM relative abundance also is slightly higher at AC4700 than at AC2000B during most of the time (Fig. 5c).

The lowermost canyon trap AC4700 is the one showing the highest relative content of $CaCO_3$ (Fig. 5b and Table 1), with the most prominent peak occurring in June 2012. The fact that this $CaCO_3$ peak is synchronous with OM and opal peaks (Fig. 5 b-d) following three months of rather high primary production (Fig. 7) points to pelagic sedimentation of material derived from the spring phytoplanktonic bloom. This view is further supported by a relative high presence of foraminifera and pteropod shells in trap samples, which evidences a significant contribution of biogenic carbonate particles. Berner and Honjo (1981) reported a ~12% contribution of pteropod shells to the total carbonate flux in open ocean sites of the Atlantic Ocean. Given that labile organic material can be degraded while being transported to lower canyon environments (de Stigter et al., 2007; Pasqual et al., 2011), the higher $CaCO_3$ relative abundance at AC4700 probably results from a good preservation of pelagic carbonate shells. Furthermore, N:OC ratios also point to a marine, pelagic origin. It is to be noted that the calcium carbonate compensation depth (CCD) in the region is several hundred meters

deeper (~5200 m) than the deployment depth of our deeper trap AC4700 (Biscaye et al., 1976), which prevents sensible dissolution of $CaCO_3$ particles. Also some contribution of terrestrial, river-sourced $CaCO_3$ cannot be totally discarded, as Nalón River drains onto limestone formations and advection processes might bring light carbonate particles to the outer continental margin.

Compared to other locations in the Bay of Biscay, peaks in TMFs in the upper open slope west of the Avilés Canyon (WS1200) are higher than, for instance, those recorded by Schmidt et al. (2009) in the western slope adjacent to the nearby Cap Ferret submarine canyon. Similarly, TMFs peaks in AC2000T and AC2000B are also higher than those recorded both in the water column (1350 m water depth, 950 m above the bottom) and near-bottom (at 2250 m water depth, 50 m above the bottom) by Heussner et al. (1999) in the mid Cap Ferret Canyon at 2300 m of water depth, where neither variability in river discharge nor in wind dynamics (see Section 5.2.1) seem to be related to the observed rapid changes (e.g. from 57 mg m^{-2} d^{-1} to 2630 mg m^{-2} d^{-1}) in particulate fluxes. Instead, variability in particle fluxes in the mid Cap Ferret Canyon seems to be mainly controlled by oceanographic forcing, namely short-term fluctuations of the along-slope current (Heussner et al., 1999). The links of atmospheric, oceanographic and other forcings with particle fluxes in the Avilés Canyon area are discussed in the next chapter.

5.2 Physical controls on particle fluxes
5.2.1 Storms

Increased wave height due to storms and their effects on the water column and on the resuspension of seabed sediments seem to be the main driver of TMFs temporal variability in the Avilés submarine canyon. This is supported by the good correlation coefficients (~0.6-0.7) of TMFs with wave height and wind speed at time lag 1 (15 days) for AC2000T and AC2000B (see section 4.3), which also indicates that in terms of sediment dynamics the middle reaches of the Avilés Canyon respond relatively quick (15 days) to external forcings such as waves and wind. Given its shallower depth, it is to be supposed that the upper canyon reaches respond even faster. Such relationship is in agreement with observations made by several authors who have shown that submarine canyons ease the transport of particulate matter from coastal and shelf environments to the deep sea, often during storms associated to large wave heights and subsequent current intensification (Guillén et al., 2006; Palanques et al., 2008, 2009; Ulses et al., 2008b; Sànchez-Vidal et al., 2012). Other authors have also pointed

out that in some continental margins, particles from the shelf reach the deep margin and basin after experiencing several cycles of deposition and resuspension (e.g. Palanques et al., 2012; Rumín-Caparrós et al., 2013).

The equally good correlation (~0.7) of both levels of AC2000 with total river discharge means that riverine inputs have a clear impact on TMFs in the Avilés Canyon mid course, although with some delay as this coefficient corresponds to time lag 3 (45 days). Several storm events occurred during the monitoring period. The first event took place in early March 2012 after a February increase in riverine discharge up to almost 1100 m^3 s^{-1} (Fig. 3a), which likely resulted in the arrival of large amounts of particulate matter to the shelf. During this event, easterly winds up to 12 m s^{-1} (Fig. 3c, d) co-occurred with up to 6 m Hs swell waves from the NW-N quadrant reaching the study area (grey shaded area in Fig. 3e, f). The combination of easterly winds and high swell waves led to a surficial westward shelf current peaking at 37 cm s^{-1} (grey shaded areas in Figs. 3g, h), involving a westwards and seawards transport of particles in the surface Ekman layer. This situation favoured the surface advection and subsequent settling of particulate matter originating from the shelf into the Avilés Canyon down to depths of at least 2000 m eventually reaching also the open slope to the west towards La Vallina branches (Figs. 1, 2 and 4a). However, the transport in the bottom Ekman layer, should favour a shoreward flow thus hampering the bottom nepheloid layer to reach the shelf edge and beyond. The opposite situation occurred during the April 2012 and the late January-early February 2013 storm (see further down). This points out to the relative importance of surface nepheloid layer transport vs. bottom nepheloid layer transport under different situations. The above-described scenario explains why no significant LFs were recorded in AC2000B and WS12000 in March 2012 (Fig. 4d, e). It is worth referring here to the discrepancies between sediment trap-based vertical mass TMFs and turbidity sensor-based LFs (Fig. 4). This topic has been discussed often in the literature where discrepancies are attributed to the inefficiency of sediment traps to collect laterally advected particulate matter under high current speeds, and also to the presence of coarse particles that settle rapidly and give low turbidity readings (e.g. Gardner, 1989; Gardner and Walsh, 1990; Walsh and Gardner, 1992; Bonnin et al., 2008). The lack of data on the sizes of suspended sedimentary particles in our study area prevents us to further discuss this aspect.

The weaker correlation (~0.4-0.5) of TMFs during the studied period and the three variables considered in Table 3 for the near-bottom, western open slope trap WS1200, jointly with its fit with time lag 2 (30 days) for wave height and wind speed and time lag

4 (60 days) for total river discharge points to a different behaviour of the canyon and the upper open slope west of it. This also implies that, if affected by advection from the shelf, the open upper slope west of the Avilés Canyon will be impacted with a noticeable delay (eventually involving shifts in the meteoceanic conditions) and to a lesser extent than the Avilés Canyon mid (and probably upper) course.

A second, more severe storm was recorded in late April 2012, which was practically concomitant with a >600 m^3 s^{-1} peak in riverine discharge (Fig. 3a) bringing river-sourced particles to the shelf. During this storm, western wind bursts of 17.1 m s^{-1} (Fig. 3c, d) were accompanied by an 8-day period of waves from the northwest (light brown shaded areas in Fig. 3e) exceeding 8 m of Hs (Fig. 3f) that may have caused again shelf sediment resuspension adding to river-sourced inputs. Prevailing wind-driven surficial eastward shelf currents (light brown shaded areas in Fig. 3g, h) opposed to the arrival of shelf resuspended settling particles within the surface Ekman layer into the Avilés Canyon and its western open slope. It is noteworthy that during this storm an increase in raw near-bottom current speed up to 34 cm s^{-1} occurred at AC2000B (Fig. 9). Filtered current speed also increased in WS1200, reaching a peak value of 10.8 cm s^{-1}. However, filtered current speed in AC2000B remained greatly unchanged despite the large increment of the raw velocity data. A possible supporting evidence of some near-bottom advection of particles during the April 2012 event is the small LFs spike in AC2000B. This suggests that part of the material supplied by the river and eventually resuspended from the shelf floor could have been transported offshore in the bottom Ekman layer having an impact initially restricted to the canyon upper and mid courses, which may explain the increase in LFs recorded in AC2000B (Fig. 4e). The lack of a concurrent increase in LFs in WS1200 is in agreement with the view of a different behaviour of the upper open slope compared to the canyon.

The concurrent though smaller peak of TMF in April 2012 at AC2000T (mid-water) is tentatively attributed to intermediate nepheloid layers detaching from the canyon head and upper course, or from the upper continental slope. Nepheloid layers spreading along isopycnal surfaces have been found at intermediate depths over the continental slope of the nearby Celtic Sea, where near-bottom nepheloid layers have been identified too (e.g. McCave et al., 2001). Several studies demonstrate that such nepheloid layers mainly result from particle resuspension triggered by storms associated to high waves and increased bottom currents, with internal waves eventually playing a role in such particle loading (e.g. Biscaye and Anderson, 1994; Durrieu de Madron et al., 1999; Bonnin et al., 2002; Puig et al., 2004b).

In an attempt to asses if sedimentary particles could be carried from the mid to the lowermost canyon reaches we built the progressive vector diagram in figure 10 using near-bottom raw (non-filtered) currents recorded at the location of AC2000B (near-bottom). We selected the period of April-May 2012 as it corresponds to the highest TMFs in the canyon the canyon mid course and also includes a significant storm and river discharge event, so that it could be considered representative of enhanced along canyon transport. We also assume that the overall circulation pattern in the upper-middle canyon course (as represented by station AC2000) could be extrapolated to the canyon lowermost course. The composition depicted in figure 10 therefore represents the horizontal displacement that a particle should follow if the horizontal current field was homogenous in the study area. The plot shows that particles which on the 1st of April 2012 were at ~2000 m depth on the position of mooring AC2000 (AC2000B at 44 mab) could move horizontally roughly following the direction of the canyon from AC2000 to AC4700, and reach the position of AC4700 (still at ~2000 m depth) around the 10th of May 2012. This scenario fits with the pattern of increments in TMFs in both stations, first in AC2000 in April 2012, and 30 days later in AC4700 (Fig. 4b-c). However, these results and their interpretation have to be taken with care, as the characteristics of the near bottom transit of particles would depend on the deeper circulation of Avilés Canyon, not necessarily connected to the circulation at upper layers. The non-significance of cross-correlation coefficients between AC4700 and the external forcings in Table 3 points towards a different behaviour of the lowermost canyon compared to the shallower canyon reaches and open upper slope.

The significance of residual currents that can be derived from the hodograph in figure 10 is discussed further down within section 5.2.2 on tidal currents.

A set of moderate storms with Hs never exceeding 5.4 m occurred from October to December 2012 (Fig. 3f). During this period, prevailing westerly winds (Fig. 3c) triggering eastward coastal currents (Fig. 3g) led to bottom Ekman transport directed offshore, likely contributing to the particle loading of bottom nepheloid layers in the mid and outer shelf and advecting particles in suspension towards the Avilés Canyon head, which were carried subsequently into the canyon upper and middle sections, as recorded by the progressive increase in TMF at AC2000B (near-bottom) (Fig. 4b). The fact that a slight increase in TMF is also observed at AC2000T suggests that in addition to the bottom nepheloid layer also intermediate nepheloids eventually detaching from the upper canyon and/or slope reached the location of AC2000 mooring

station in the middle canyon (Fig. 4b). Durrieu de Madron et al. (1990) found that nepheloid structures extending seaward along isopycnals in the Gulf of Lion may increase the frequency of injection of sediment to the water column over the continental slope and sediment fluxes along submarine canyons.

The last stormy period with an impact on particle fluxes in the Avilés Canyon and the adjacent slope to the west lasted 27 days in January and February 2013. That event started synchronously with an increase in discharge of the Nalón River exceeding 800 m^3 s^{-1}, which likely resulted in the arrival of large amounts of material to the continental shelf (Fig. 3a). During this stormy period, westerly winds of about 18 m s^{-1} blowing along the Cantabrian coast raised waves up to 7.5 m of Hs arriving from the northwest (brown shaded areas in Fig. 3c-f), induced downwelling pulses (Fig. 8) and promoted an eastward Ekman surface transport (Fig. 6a). However, the eastward coastal currents that these wind conditions generate along the shelf might also lead to bottom Ekman transport directed offshore, potentially advecting sediments into the canyon head and slope as indicated by LF increases up to 1.97 and 0.61 g m^{-2} s^{-1} in AC2000B and WS1200, respectively (Fig. 4d, e).

Unlike the storm of late April 2012, this one was not accompanied by an increase in near-bottom filtered current speed in WS1200 (Fig. 9a), where the current meter provided negligible low-passed Godin $(A^2A_{25})/(24^225)$ currents (Godin, 1972), likely because it fell in a gully during the second deployment period from September 2012 to March 2013, thus lying in the shadow of along-slope currents. A 70 m larger deployment depth during the second period compared to the first deployment period supports this view. Noticeably, raw near-bottom current speed (amplitude of tidal currents) reached the highest value (39 cm s^{-1}) in late January 2013 in WS1200. However, the location of the mooring obscures establishing the link between this increase and the passage of the stormy period here described.

Vertical TMFs also augmented in AC2000B during the occurrence of the January-February 2013 storm and shortly after up to a maximum of 5.24 g m^{-2} d^{-1} by mid-February, following the above-mentioned increase in LFs in January (Fig. 4b, e). Within this stormy period, filtered currents were also rather low in AC2000B, similarly to WS1200, while raw near-bottom currents were fluctuating markedly around a mean value close to 22 cm s^{-1}, peaking at 37 cm s^{-1} (Fig. 9a, c). The increase in LFs and TMFs at AC2000B is interpreted as indicative of the arrival to the mid Avilés Canyon of bottom nepheloid layers triggered by the storm and increased river discharge, which

further supports the offshore transport hypothesis in the bottom Ekman layer. The observations made also indicate that the nepheloid layers entering the canyon had practically no impact on TMFs in the open slope to the west (Fig. 4a). It is also plausible that the bottom nepheloid layer has been supplied by particles settling down from intermediate nepheloid layers. The peak values in TMFs recorded in early March 2013 at AC4700 could also be related to the transfer of the storm signal from AC2000B downcanyon (Fig. 4c). The higher contents of lithogenics at AC4700 during the second deployment period (September 2012 to March 2013) compared to the first one (March to September 2012) (Fig. 5a) support this view, as such higher values could be interpreted as a result of the set of moderate storms from October to December 2012 and the January-February 2013 storm, with concomitant increases of TMFs at AC2000B (Fig. 4b). The downcanyon propagation of bottom nepheloid layers, eventually leading to intermediate nepheloid layers too, has been noticed in other submarine canyons around Iberia, such as the Nazaré Canyon (van Weering et al., 2002; Martín et al., 2011).

The coastal downwelling conditions in early 2013, together with the concurrent increase in river discharge (Fig. 3a) and the phytoplankton bloom near Cabo Peñas and more generally along the coastal area, already visible in March 2013 (Fig. 7), help explaining the enrichment in OM and opal visible in all stations by March 2013 (Fig. 5c, d). In addition to the general hydrometeorological and hydrological conditions in the Bay of Biscay, it is likely that the new nutrients brought by the sustained high river discharge from mid-January 2013 onwards by Nalón River (Fig. 3a) and also other Cantabrian rivers (data not shown) contributed to the coastal phytoplankton bloom starting in March 2013 and continuing for the following months (Fig. 7). The overall situation would have resulted in the formation of turbid layers enriched in biogenic constituents that were spreading over the margin at various levels, eventually eased by Ekman intermediate and bottom transport, including nepheloid layers detaching from the seabed at certain depths. The impact of the OM and opal-rich turbid layers extending over the continental margin was, however, much larger at mid depths, both in the water column and near-bottom (i.e. ~1200 m of water depth) and not restricted to the canyon, as shown by the records of traps AC2000T and WS1200. This impact was much less, though it was still visible, in the deeper near-bottom traps AC2000B and AC4700 in the mid and lower canyon (Fig. 5c, d). The marine algal contribution to the particle load was especially remarkable at mid depths, as indicated by the prominent increases in the N:OC ratio at traps AC2000T and WS1200, likely resulting from downwelling and pelagic settling. Such a signal, however, barely reached the deeper

28

levels either because of consumption, dilution or retention at shallower levels (e.g. at density boundaries).

Overall, our set of observations indicates that the direction of wind, especially when it blows over a threshold of 12 m s^{-1} (Fig. 3d), and the wind-triggered currents determine whether river-contributed and resuspended shelf particulate matter reaches Avilés Canyon or not, and if this occurs mostly at surface, intermediate or near-bottom levels (Fig. 11). Clearly, there are two contrasting situations: i) during westerly wind conditions an eastward shelf circulation is established and sea surface plumes tend to pile up along the coast while the Ekman bottom transport can carry sedimentary particles offshore; and ii) during easterly wind conditions a westward shelf circulation is established and sea surface plumes can move over the canyon head and upper course while the bottom nepheloid layer would be pushed shoreward.

According to Ruiz-Villareal et al. (2004), during the upwelling season eased by the prevailing easterly winds in spring-summer, mean westward flows would enhance upwelling over the head and upper reaches of the Avilés Canyon. This situation may enhance the westwards and seawards transport of particles in the surface Ekman Layer and thus, the advection and subsequent settling of particulate matter from the shelf into the Avilés Canyon and the open continental slope west of it (Fig. 11). Following the same authors, during the downwelling season induced by the prevailing westerly winds in autumn-winter, near-bottom flows in the upper reaches of the Avilés Canyon are variable but directed offshore, which would enhance the propagation of bottom nepheloid layers from the canyon head into the canyon upper and middle sections and possibly beyond.

5.2.2 Tidal currents

The influence of tidal currents on sediment transport along submarine canyons has attracted since long the attention of researchers (e.g. Shepard et al., 1979 and references therein). Observations in the Baltimore Canyon showed how internal tides focussing in the upper and middle canyon course resulted in sediment resuspension and ultimately in a net down-canyon sediment transport (Gardner, 1989). In the Nazaré Canyon, off Portugal, de Stigter et al. (2007) demonstrated how 15-25 cm s^{-1} semidiurnal tidal currents in the upper and middle canyon course were able to trigger sudden increases in suspended particulate matter and to promote net down-canyon sediment transport.

The spectral analysis carried out in the near-bottom AC2000B and WS1200 current meters within the Avilés Canyon and on the adjacent open slope, respectively, reveals that the main tidal component is semidiurnal (M2) with frequencies of 0.0805 cycles per hour (cph) (12.42 h) (not shown). Other less energetic peaks are also present in the inertial frequency (f) of 0.0605 cph (16.52 h), as a mix of diurnal species (mostly K1) with 0.0410 cph (24.38 h), and as higher harmonic species M4 and M6 with 0.1621 cph (6.17 h) and 0.2441 cph (4.10 h), respectively. This underlines the relevance of tidal currents in the dynamics of the upper and middle Avilés Canyon and its adjacent slope. The Godin $(A^2A_{25})/(24^225)$ filter applied to obtain tidal period variations and extract subinertial series shows that tidal currents represented, at least, 60% in average of all currents recorded both at Avilés Canyon and on the open continental slope west of it during the study period.

One further aspect that can be derived from the currentmeter time series, and is well depicted in the hodograph of figure 10, is the existence of two directions of polarization of the residual current at AC2000B. In a first time the current measured at that depth consisted in a residual movement towards NW (hodograph ending at about 5km North/5 km West), so suggesting the presence of a residual current coming downcanyon along the Avilés Canyon axis. Then the residual movement due to horizontal currents at AC2000B becomes directed towards NE (hodograph end at about 10 km North/3km East). This would imply the presence at AC2000B, during this period, of a current coming from the slope southwest of the mooring position and directed towards NE roughly. This would be a residual current coming from La Vallina tributary branches located in the westward flank of Avilés Canyon (Figs. 1 and 2). In evolution that follows, periods when this residual current was flowing down-canyon coming from the Avilés Canyon axis can be distinguished from periods (that seem to predominate) when the residual current came from La Vallina branches.

During the entire period there were also short-lived current fluctuations overprinted on these residual currents, which are apparently polarized along the Avilés Canyon axis. These short period fluctuations have periods from half a day (that would be the semidiurnal tidal currents) to one or two days and the particle excursions associated with these movements seem to align very well with the orientation of the Avilés Canyon axis no matter the orientation of the residual flow.

Tidal currents add, therefore, an extra amount of energy to the prevailing bottom currents, which may actively favour sediment transport along the Avilés submarine canyon system. Repeated cycles of semidiurnal tides shorten the intervals during which particles settle, thus contributing to keep a permanent background of suspended particles in near-bottom waters (Fig. 4d, e), which is about 0.04 g m^{-2} d^{-1}. De Stigter et al. (2007) noticed a similar situation in the Nazaré Canyon off the western Iberian margin. Also, during quiet summer conditions when the water column is stratified the turbulence associated to internal waves likely has the capability to resuspend and remobilize sedimentary deposits on the continental slope and possibly the outer and mid-shelf (e.g. Quaresma et al., 2007).

The above observations further suggest an important role being played by the La Vallina tributary branches, in the westward flank of Avilés Canyon. The significance of these tributaries is further discussed in the next section.

5.2.3 Coastal and seafloor physiography

The interaction of the regional circulation with shoreline and seafloor morphological irregularities has been proven to influence the long-term sediment dispersal and accumulation in continental margins. In the study area, the interaction of the Cabo Peñas headland and the Avilés Canyon system topography with the wind-forced circulation adds complexity to the understanding of sediment transport.

As pointed out by DeGeest et al. (2008), headlands behave as sediment bypass areas where alongshore currents accelerate and deviate offshore. This is well illustrated, amongst other examples, by Cape Creus coastal promontory, in the Gulf of Lion, northwestern Mediterranean Sea, which accelerates and deviates shelf water flows offshore into the Cap de Creus Canyon (Canals et al., 2006; Lastras et al., 2007; Ulses et al., 2008a). Cabo Peñas headland (Fig. 1) might play a similar a role, i.e. deflecting and accelerating the regional along shelf circulation, thus conveying sediment off the nearshore belt into the Avilés Canyon. This would be associated with the specific interactions of Cabo Peñas promontory, and also the canyon head, with the prevailing westward and eastward shelf and slope surface circulation favouring coastal upwelling and downwelling, respectively (see sections 2 and 5.2.1).

Based on morphological criteria, La Vallina tributary branches seem to play a relevant role in feeding the Avilés Canyon. After the canyon head, the heads of this set of

31

tributaries are the most indented into the continental shelf west of Cabo Peñas (Fig. 1). Therefore, they might be able to capture sediment fluxes reaching the outer shelf. Interestingly, the main La Vallina branches but the westernmost one are markedly asymmetric with dominantly smoothened right flanks and gullied left flanks (Fig. 2a-c). The westernmost branch, which is the largest and most open one, displays a similar smoothening in both flanks (Fig. 2b). These features suggest preferential sediment deposition on the right flanks of the shelf-indented La Vallina branches, with a more widespread sedimentation over the larger westernmost branch. Furthermore, the dominant gullied character of the left flanks of La Vallina branches (Fig. 2c) points to erosion. Such features might be related not only to the location of La Vallina branches but also to recirculation induced by Cabo Peñas Promontory and topographic effects caused by the presence of the head of the Avilés Canyon under the two dominant wind regimes and the associated Ekman transport at various depth levels. The sedimented, smoothened character of the shelf-indented segments of the right (eastern) flank of several of the La Vallina branches points to a significant role of the bottom Ekman transport during periods of persistent eastward shelf circulation. Part of the sediment captured by La Vallina branches likely ends up into the Avilés Canyon main trunk up-course of the location of our AC2000 mid-canyon mooring. Therefore, this set of tributaries may constitute a relevant side sediment source opening directly into the Avilés Canyon mid-course.

In situ inspection with towed cameras have shown the rough, rocky and sediment-starved nature of the Avilés Canyon head (Sánchez-Delgado et al., 2014), which on one side indicates that sedimentary particles do not settle possibly due to the prevailing intense hydrodynamics occurring there and, on another side, reinforces the role of the La Vallina branches as significant sediment feeders of the canyon mid-course. This is supported by observations made by Sánchez et al. (2014) in the neighboring La Gaviera Canyon (Fig. 1), where the intensification of hydrodynamic activity at the very canyon head is a consequence of the regional circulation, especially during high-energy events such as storms, and the semidiurnal tidal cycle causing bore-like structures and strong resuspension.

The two main directions of polarization depicted in Figure 10 illustrate the swinging behaviour of residual currents at AC2000B, with periods of northwestward residual movement followed by periods of northeastward movement and so on (see section 5.2.2). These directions correspond to residual currents flowing down the main trunk of the Avilés Canyon alternating with currents coming from La Vallina branches, and

therefore further support the significant role of La Vallina tributaries in the dynamics and sediment fluxes of the Avilés Canyon system.

The smaller tributaries situated between la Vallina group and the main canyon head do not look particularly asymmetric in terms of flank smoothening and gullies appear only locally, without forming closely spaced sets as in some of the flanks of la Vallina branches (Fig. 1). Their overall appearance also suggests some sediment smoothening, although not as pronounced as in the shelf-indented segments of the (mostly right) flanks of La Vallina branches, which could be related to the shorter incision distance into the continental shelf of these smaller tributaries, subsequently resulting in a lessened ability to capture sediment escaping from the shelf, but also to an extended effect of the intense hydrodynamics in the main canyon head preventing particles to settle, as described above.

5.2.4 Bottom trawling

The role of bottom trawling in resuspending sediments and inducing sediment gravity flows within submarine canyons has been documented by several authors, in particular in La Fonera Canyon, in the northwestern Mediterranean Sea (Palanques et al., 2006b; Martín et al., 2008; Puig et al., 2012; Martín et al., 2014a, b). These authors have shown how the action of trawlers on the seabed triggers sharp near-bottom turbidity peaks associated with increases in downslope near-bottom currents. Amongst other authors, Pusceddu et al. (2014) and Martín et al. (2015) have investigated other far-reaching consequences of recurrent bottom trawling.

In the western slope adjacent to Avilés Canyon there is an active commercial bottom trawling fishery down to 600 m of water depth that mainly targets blue whiting (Sánchez-Delgado et al., 2014, their figure 8.2.5A). As shown by satellite-based vessel tracking data (Sánchez-Delgado et al., 2014), this fishery mainly operates during periods of fair weather by means of pair trawling, a highly aggressive fishing technique able to resuspend large amounts of unconsolidated bottom sediment. An impact of bottom trawling on the Avilés Canyon area, and especially on the canyon head and upper course but also on the adjacent upper open slope is, therefore, likely. This view is supported by the increase in LFs at WS1200 (near-bottom) (Fig. 4d, grey dashed lines) during the calm seas period extending from June to September 2012, when some prominent peaks were also noticed (Fig. 4d, black solid lines). Unfortunately, there are no TMF or LF data available that could help assessing the impact of bottom

trawling in the canyon head and upper course. The bottom trawl triggered resuspension does not seem to reach the middle canyon where AC2000 was deployed (Fig. 4b).

6. Conclusions

The dominance of lithogenics (averaged annual values between 53.05-66.98% of TMFs) in settling particulate matter shows that riverine inputs represent the main source of particles arriving into the Avilés Canyon and its adjacent open slope. However, we did not detect a univocal direct control of river discharge on the temporal variability of TMFs neither in the middle and lower course of the Avilés Canyon, nor in the open upper slope west of the canyon, which suggests that other factors should control particle fluxes beyond the continental shelf edge. Indeed, certain hydrodynamic processes such as storms involve enough energy to enhance the transport of particles from coastal and shelf environments beyond that boundary.

Marine primary production is the second main source of sedimentary particles settling down in the study area. Biological components represented in average more than 30% in weight of the particles collected at all sediment traps during the monitoring period. In the lowermost canyon course (station AC4700) the $CaCO_3$ content of the biogenic fraction reaching the seabed is higher due to an enhanced flux of carbonate particles compared to siliceous ones. Furthermore, a CCD deeper (~5200 m) than our deepest sediment traps prevents significant dissolution of $CaCO_3$ particles.

Two different particle settling regimes have been identified. The first involves the shallower sediment traps in the open slope to the west (WS1200, near-bottom) and in the middle canyon course (AC2000T, mid-water). This regime encompasses a clear seasonal signal with relatively high contents of biogenic particles. The second regime refers to the deeper, near-bottom traps in the canyon middle (AC2000B) and lowermost (AC4700) course, where no seasonal signal has been identified. Instead, resuspended, lithogenic-rich particulate matter diluting biogenic particles characterizes this regime. The 16 to 30 days of delay in biogenic fraction increases recorded between the mid water AC2000T trap and the near-bottom AC2000B trap in the middle canyon course indicate some degree of connection through pelagic settling between different depth levels within the Avilés Canyon. Furthermore, the trajectory of particles between AC2000B in the middle canyon course and AC4700 in the lowermost canyon course points to an effective horizontal along canyon transport, at least at the depth

level of AC2000B. However, this does not prove that the near-bottom circulation on Avilés Canyon is connected to the circulation at upper layers.

Storms are the main physical driver of particle fluxes in the Avilés Canyon area. Wind direction and wind-driven currents determine whether resuspended shelf particulate matter may reach the canyon, and if this will occur by surface or bottom transport. Winds blowing from the west induce an onshore surface Ekman transport that pushes river-sourced and shelf-resuspended sedimentary particles away from the Avilés canyon head and upper course. However, under the same situation, the bottom Ekman transport is directed offshore and, therefore, favours the injection of particles into the Avilés Canyon. In contrast, winds blowing from the east induce coastal upwelling and favour the advection in the surface layer of particulate matter towards the Avilés Canyon and the adjacent western open slope. The same wind forcing triggers a bottom Ekman transport easing the retention of resuspended sediments on the shelf.

The Avilés Canyon head displays a very rough topography and a sediment-starved character. We suggest this to be caused, at least partly, by current deflection and turbulence induced by Cabo Peñas promontory. Such current deflection causes the bypass of suspended material over the Avilés Canyon head while steering the collection and funnelling of sediment fluxes into the main trunk of the canyon through La Vallina branches further west, as suggested by the smoothened nature of the shelf-incised segments in the right flanks of these set of tributaries, which could also respond to bottom trawling resuspension and subsequent setting there. The enhancement of hydrodynamic activity at the canyon head associated to high-energy events and tides likely plays a role too in making it sediment-starved.

Tidal currents actively contribute to sediment transport both in the upper-middle canyon course and over the western open slope. Repeated cycles of semidiurnal tides prevent particles to settle, thus resulting in a permanent background of suspended particles in near-bottom waters.

Increases in LFs occurring in summer months under calm sea conditions with no apparent relationship with meteoceanic external forcings are hypothesized to be also a consequence of commercial bottom trawling in the area. This anthropogenic disturbance may intensify the input of suspended matter all over the slope adjacent to the Avilés Canyon, and sporadically trigger shelf-slope sediment flows.

Finally, the specific physiography and orientation of the central Cantabrian margin, with a narrow continental shelf ahead of the Avilés Canyon and the presence of the nearby major coastal promontory of Cabo Peñas might help explaining its sensitivity to atmospheric and associated oceanographic forcings. The impact of these forcings on shallow waters would trigger a direct response propagating across the margin, which may explain the higher TMFs peaks in the Avilés Canyon compared to other canyons in the Bay of Biscay, such as Cap Ferret Canyon.

Acknowledgements

References

Álvarez Fanjul, E., Alfonso, M., Ruiz, M.I., López, J.D., Rodríguez, I., 2003. Building the European Capacity in Operational Oceanography, Proceedings of the Third International Conference on EuroGOOS. Elsevier Oceanogr. Ser. 69, 398-402.

Arzola, R.G., Wynn, R.B., Lastras, G., Masson, D.G., Weaver, P.P.E., 2008. Sedimentary features and processes in the Nazaré and Setúbal submarine canyons, west Iberian margin. Mar. Geol. 250, 64-88.

Asper, V.L., 1987. Measuring the flux and sinking speed of marine snow aggregates. Deep-Sea Res. Part A Oceanogr. Res. Pap. 34, 1-17.

Baines, P.G., 1982. On internal tide generation models. Deep-Sea Res. Part A Oceanogr. Res. Pap. 29, 307-338.

Baker, E.T., Milburn, H.B., Tennant, D.A., 1988. Field assessment of sediment trap efficiency under varying flow conditions. J. Mar. Res. 46, 573-592.

Bakun, A., 1973. Coastal upwelling indices, west coast of North America, 1946-71. US. Dep. Comm. NOAA. Tech. Rep. NMFS-SSRF 671.

Behrenfeld, M.J., Falkowski, P.G., 1997. Photosynthetic rates derived from satellite-based chlorophyll concentration. Limnol. Oceanogr. 42, 1-20.

Berner, R. A., Honjo, S., 1981. Pelagic Sedimentation of Aragonite: Its Geochemical Significance. Science 211, 940-942.

Biscaye, P.E., Kolla, V., Turekian, K.K., 1976. Distribution of calcium carbonate in surface sediments of the Atlantic Ocean. J. Geophys. Res. 81, 2595-2603.

Biscaye, P.E., Andersson, R.F., 1994. Fluxes of particulate matter on the slope of the southern Middle Atlantic Bight : SEEP-II. Deep-Sea Res. Part II Top. Stud. Oceanogr. 41, 459-509.

Bonnin, J., Van Raaphorst, W., Brummer, G.J., Van Haren, H., Malschaert, H., 2002. Intense mid-slope resuspension of particulate matter in the Faeroe-Shetland Channel: short-term deployment of near-bottom sediment traps. Deep-Sea Res. Part I Oceanogr. Res. Pap. 49, 1485-1505.

Bonnin, J., Heussner, S., Calafat, A., Fabrés, J., Palanques, A., Durrieu de Madron, X., Canals, M., Puig, P., Avril, J., Delsaut, N., 2008. Comparison of horizontal and downward particle fluxes across canyons of the Gulf of Lions (NW Mediterranean): Meteorological and hydrodynamical forcing. Cont. Shelf Res. 28, 1957-1970.

Botas, J.A., Fernández, E., Bode, A., Anadón, R., 1989. Water masses off the central Cantabrian coast. Sci. Mar 53, 755-761.

Buesseler, K.O., Antia, A.N., Chen, M., Fowler, S.W., Gardner, W.D., Gustafsson, O., Harada, K., Michaels, A.F., Rutgers van der Loeff, M., Sarin, M., Steinberg, D.K., Trull, T., 2007. An assessment of the use of sediment traps for estimating upper ocean particle fluxes. J. Mar. Res. 65, 345-416.

Cacchione, D.A., Pratson, L.F., Ogston, A.S., 2002. The shaping of continental slopes by internal tides. Science, 296, 724-727.

Canals, M., Puig, P., de Madron, X.D., Heussner, S., Palanques, A., Fabrés, J., 2006. Flushing submarine canyons. Nature 444, 354-7.

Canals, M., Company, J.B., Martín, D., Sànchez-Vidal, A., Ramírez-Llodra, E., 2013. Integrated study of Mediterranean deep canyons: Novel results and future challenges. Prog. Oceanogr. 118, 1-27.

Charria, G., Lazure, P., Le Cann, B., Serpette, A., Reverdin, G., Louazel, S., Batifoulier, F., Dumas, F., Pichon, A., Morel, Y., 2013. Surface layer circulation derived from Lagrangian drifters in the Bay of Biscay. J. Mar. Syst. 109, S60-S76.

DeGeest, A.L., Mullenbach, B.L., Puig, P., Nittrouer, C.A., Drexler, T.M., Durrieu de Madron, X., Orange, D.L., 2008. Sediment accumulation in the western Gulf of Lions, France: the role of Cap de Creus canyon in linking shelf and slope sediment dispersal systems. Cont. Shelf Res. 28, 2031-2047.

De Leo, F.C., Smith, C.R., Rowden, A.A., Bowden, D.A., Clark, M.R., 2010. Submarine canyons: hotspots of benthic biomass and productivity in the deep sea. Proc. R. Soc. B Biol. Sci. 277, 2783-2792.

de Stigter, H.C., Boer, W., de Jesus Mendes, P. a., Jesus, C.C., Thomsen, L., van den Bergh, G.D., van Weering, T.C.E., 2007. Recent sediment transport and deposition in the Nazaré Canyon, Portuguese continental margin. Mar. Geol. 246, 144-164.

de Stigter, H.C., Jesus, C.C., Boer, W., Richter, T.O., Costa, A., van Weering, T.C.E., 2011. Recent sediment transport and deposition in the Lisbon-Setúbal and Cascais submarine canyons, Portuguese continental margin. Deep-Sea Res. Part II Top. Stud. Oceanogr. 58, 2321-2344.

Díaz del Río, G., González, N., Marcote, D., 1998. The intermediate Mediterranean water inflow along the northern slope of the Iberian Peninsula. Oceanol. Acta 21, 157-163.

Dickson, R.R., Gould, W.J., Müller, T.J., Maillard, C., 1985. Estimates of the mean circulation in the deep (> 2,000 m) layer of the Eastern North Atlantic. Prog. Oceanogr. 14, 103-127.

Drake, D.E., Gorsline, D.S., 1973. Distribution and transport of suspended particulate matter in Hueneme, Redondo, Newport and La Jolla submarine canyons. Geol. Soc. Am. Bull. 84, 3949-3698.

Durrieu de Madron, X., Nyffeler, F., Godet, C.H.C., 1990. Hydrographic structure and nepheloid spatial distribution in the Gulf of Lions continental margin. Cont. Shelf Res. 10, 915-929.

Durrieu de Madron, X., 1994. Hydrography and nepheloid structures in the Grand-Rhône canyon. Cont. Shelf Res. 14, 457-477.

Durrieu De Madron, X., Castaing, P., Nyffeler, F., Courp, T., 1999. Slope transport of suspended particulate matter on the Aquitanian margin of the Bay of Biscay. Deep-Sea Res. Part II 46, 2003-2027.

Fabrés, J., Calafat, A., Sànchez-Vidal, A., Canals, M., Heussner, S., 2002. Composition and spatio-temporal variability of particle fluxes in the Western Alboran Gyre, Mediterranean Sea. J. Mar. Syst. 34, 431-456.

Fanjul, E.A., Gómez, B.P., Sánchez-Arévalo, I.R., 1997. A description of the tides in the Eastern North Atlantic. Prog. Oceanogr. 40, 217-244.

Fernández, E., Bode, A., 1991. Seasonal patterns of primary production in the Central Cantabrian Sea (Bay of Biscay). Sci. Mar. 55, 629-636.

Fernández, E., Bode, A., 1994. Succession of phytoplankton assemblages in relation to the hydrography in the southern Bay of Biscay: A multivariate approach. Sci. Mar. 58, 191-205.

39

Friocourt, Y., Levier, B., Speich, S., Blanke, B., Drijfhout, S.S., 2007. A regional numerical ocean model of the circulation in the Bay of Biscay. J. Geophys. Res. Ocean. 112, 1-19.

Frouin, R., Fiúza, A.F.G., Ambar, I., Boyd, T.J., 1990. Observations of a poleward surface current off the coasts of Portugal and Spain during winter. J. Geophys. Res. Ocean. 95, 679-691.

Gardner, W.D., 1985. The effect of tilt on sediment trap efficiency. Deep-Sea Res. Part A Oceanogr. Res. Pap. 32, 349-361.

Gardner, W.D., 1989. Baltimore Canyon as a modern conduit of sediment to the deep sea. Deep-Sea Res. Part A Oceanogr. Res. Pap. 36, 323-358.

Gardner, W.D., Walsh, I.D., 1990. Distribution of macroaggregates and fine-grained particles across a continental margin and their potential role in fluxes. Deep-Sea Res. Part A Oceanogr. Res. Pap. 37, 401-411.

Gardner, W.D., Biscaye, P.E., Richardson, M.J., 1997. A sediment trap experiment in the Vema Channel to evaluate the effect of horizontal particle fluxes on measured vertical fluxes. J. Mar. Res. 55, 995-1028.

Gil, J., Gomis, D., 2008. The secondary ageostrophic circulation in the Iberian Poleward Current along the Cantabrian Sea (Bay of Biscay). J. Mar. Syst. 74, 60-73.

Gili, J., Bouillon, J., Palanques, A., Puig, P., 1999. Submarine canyons as habitats of prolific plankton populations: three new deep-sea Hydroidomedusae in the western Mediterranean. Zool. J. Linn. Soc. 125, 313-329.

Godin, G., 1972. The analysis of tides, 264 pp. Univ. Toronto. Toronto, Canada.

Gómez-Ballesteros, M., Druet, M., Muñoz, A., Arrese, B., Rivera, J., Sánchez, F., Cristobo, J., Parra, S., García-Alegre, A., González-Pola, C., Gallástegui, J., Acosta, J., 2013. Geomorphology of the Avilés Canyon System, Cantabrian Sea (Bay of Biscay). Deep-Sea Res. Part II Top. Stud. Oceanogr. 1-19.

González-Pola, C., Ruiz-Villarreal, M., Lavín, A., Cabanas, J.M., Álvarez-Fanjul, E., 2005. A subtropical water intrusion spring-event in the shelf-slope of the south-western Bay of Biscay after strong wind-forcing pulses. J. Atmos. Ocean Sci. 10, 343-359.

González-Pola, C., Fernández-Díaz, J.M., Lavín, A., 2007. Vertical structure of the upper ocean from profiles fitted to physically consistent functional forms. Deep-Sea Res. Part I Oceanogr. Res. Pap. 54, 1985-2004.

González-Quirós, R., Cabal, J., Álvarez-Marqués, F., Isla, A., 2003. Ichthyoplankton distribution and plankton production related to the shelf break front at the Avilés Canyon. ICES J. Mar. Sci. 60, 198-210.

Guillén, J., Palanques, A., Puig, P., Durrieu de Madron, X., Nyffeler, F., 2000. Field calibration of optical sensors for measuring suspended sediment concentration in the western Mediterranean. Sci. Mar. 64, 427-435.

Guillén, J., Bourrin, F., Palanques, A., Durrieu de Madron, X., Puig, P., Buscail, R., 2006. Sediment dynamics during wet and dry storm events on the Têt inner shelf (SW Gulf of Lions). Mar. Geol. 234, 129-142.

Haynes, R., Barton, E.D., 1990. A poleward flow along the Atlantic coast of the Iberian Peninsula. J. Geophys. Res. Ocean. 95, 11425-11441.

Heussner, S., Ratti, C., Carbonne, J., 1990. The PPS 3 time-series sediment trap and the trap sample processing techniques used during the ECOMARGE experiment. Cont. Shelf Res. 10, 943-958.

Heussner, S., Durrieu de Madron, X., Radakovitch, O., Beaufort, L., Biscaye, P.E., Carbonne, J., Delsaut, N., Etcheber, H., Monaco, A., 1999. Spatial and temporal patterns of downward particle fluxes on the continental slope of the Bay of Biscay (northeastern Atlantic). Deep-Sea Res. II 46, 2101-2146.

Heussner, S., Durrieu de Madron, X., Calafat, A., Canals, M., Carbonne, J., Delsaut, N., Saragoni, G., 2006. Spatial and temporal variability of downward particle fluxes on a continental slope: Lessons from an 8-yr experiment in the Gulf of Lions (NW Mediterranean). Mar. Geol. 234, 63-92.

Hickey, B., Baker, E., Kachel, N., 1986. Suspended particle movement in and around Quinault submarine canyon. Mar. Geol. 71, 35-83.

Hung, J.-J., Lin, C.-S., Chung, Y.-C., Hung, G.-W., Liu, W.-S., 2003. Lateral fluxes of biogenic particles through the Mien-Hua canyon in the southern East China Sea slope. Cont. Shelf Res. 23, 935-955.

Iorga, M.C., Lozier, M.S., 1999a. Signatures of the Mediterranean outflow from a North Atlantic climatology: 1. Salinity and density fields. J. Geophys. Res. 104, 25985-26009.

Iorga, M.C., Lozier, M.S., 1999b. Signatures of the Mediterranean outflow from a North Atlantic climatology: 2. Diagnostic velocity fields. J. Geophys. Res. Ocean. 104, 26011-26029.

Jouanneau, J.-M., Weber, O., Champilou, N., Cirac, P., Muxika, I., Borja, A., Pascual, A., Rodríguez-Lázaro, J., Donard, O., 2008. Recent sedimentary study of the shelf of the Basque country. J. Mar. Syst. 72, 397-406.

Lastras, G., Canals, M., Urgelès, R., Amblàs, D., Ivanov, M., Droz, L., Dennielou, B., Fabrés, J., Schoolmeester, T., Akhmetzhanov, A., Orange, D., García-García, A., 2007. A walk down the Cap de Creus canyon, northwestern Mediterranean Sea: Recent processes inferred from morphology and sediment bedforms. Mar. Geol. 246, 176-192.

Lastras, G., Canals, M., Amblàs, D., Calafat, A.M., Durán, R., Muñoz, A., Pedrosa-Pàmies, R., Sànchez-Vidal, A., Rayo, X., Rumin, A., Tubau, X., Veres, O., 2012. The Avilés submarine canyon drainage system, northern Iberian margin. The Deep-Sea and Sub-Seafloor Frontiers Conf. 11-14 March, Spain, Abstr. Vol. P085.

Lavín, A., Valdés, L., Sénchez, F., Abaunza, P., Forest, A., Boucher, J., Lazure, P., Jegou, A.-M., 2006. The Bay of Biscay: the encountering of the ocean and the shelf. Seas Harvard Press 14, 933-1001.

Le Cann, B., Serpette, A., 2009. Intense warm and saline upper ocean inflow in the southern Bay of Biscay in autumn-winter 2006-2007. Cont. Shelf Res. 29, 1014-1025.

Margalef, R., 1978. Life-forms of phytoplankton as survival alternatives in an unstable environment. Oceanol. Acta 1, 493-509.

Martín, J., Palanques, A., Puig, P., 2006. Composition and variability of downward particulate matter fluxes in the Palamós submarine canyon (NW Mediterranean). J. Mar. Syst. 60, 75-97.

Martín, J., Puig, P., Palanques, A, Masqué, P., García-Orellana, J., 2008. Effect of commercial trawling on the deep sedimentation in a Mediterranean submarine canyon. Mar. Geol. 252, 150-155.

Martín, J., Palanques, A., Vitorino, J., Oliveira, A., de Stigter, H.C., 2011. Near-bottom particulate matter dynamics in the Nazaré submarine canyon under calm and stormy conditions. Deep-Sea Res. Part II Top. Stud. Oceanogr. 58, 2388-2400.

Martín, J., Puig, P., Palanques, A., Ribó, M., 2014a. Trawling-induced daily sediment resuspension in the flank of a Mediterranean submarine canyon. Deep-Sea Res. Part II Top. Stud. Oceanogr. 104, 174-183.

Martín, J., Puig, P., Masqué, P., Palanques, A., Sánchez-Gómez, A., 2014b. Impact of bottom trawling on deep-sea sediment properties along the flanks of a submarine canyon. PLoS One 9, e104536.

Martín, J., Puig, P., Palanques, A., Giamportone, A., 2015. Commercial bottom trawling as a driver of sediment dynamics and deep seascape evolution in the Anthropocene. Anthropocene 7, 1-15.

McCave, I.N., Hall, I.R., Antia, a. N., Chou, L., Dehairs, F., Lampitt, R.S., Thomsen, L., Van Weering, T.C.E., Wollast, R., 2001. Distribution, composition and flux of particulate material over the European margin at 47°-50°N. Deep-Sea Res. Part II Top. Stud. Oceanogr. 48, 3107-3139.

Miquel, J.C., Martín, J., Gasser, B., Rodríguez-y-Baena, A., Toubal, T., Fowler, S.W., 2011. Dynamics of particle flux and carbon export in the northwestern Mediterranean Sea: A two decade time-series study at the DYFAMED site. Prog. Oceanogr. 91, 461-481.

Moreno-Madriñán, M.J., Fischer, A.M., 2013. Performance of the MODIS FLH algorithm in estuarine waters: a multi-year (2003-2010) analysis from Tampa Bay, Florida (USA). Int. J. Remote Sens. 34, 6467-6483.

Mortlock, R.A., Froelich, P.N., 1989. A simple method for the rapid determination of biogenic opal in pelagic marine sediments. Deep-Sea Res. Part A Oceanogr. Res. Pap. 36, 1415-1426.

Mulder, T., Zaragosi, S., Garlan, T., Mavel, J., Cremer, M., Sottolichio, a., Sénéchal, N., Schmidt, S., 2012. Present deep-submarine canyons activity in the Bay of Biscay (NE Atlantic). Mar. Geol. 295-298, 113-127.

Nittrouer, C.A., Wright, L.D., 1994. Transport of particles across continental shelves. Rev. Geophys. 32, 85-113.

Oliveira, A., Santos, A.I., Rodrigues, A., Vitorino, J., 2007. Sedimentary particle distribution and dynamics on the Nazaré canyon system and adjacent shelf (Portugal). Mar. Geol. 246, 105-122.

Paillet, J., Mercier, H., 1997. An inverse model of the eastern North Atlantic general circulation and thermocline ventilation. Deep-Sea Res. Part I Oceanogr. Res. Pap. 44, 1293-1328.

Palanques, A., El Khatab, M., Puig, P., Masqué, P., Sánchez-Cabeza, J.A., Isla, E., 2005. Downward particle fluxes in the Guadiaro submarine canyon depositional system (north-western Alboran Sea), a river flood dominated system. Mar. Geol. 220, 23-40.

Palanques, A., Durrieu de Madron, X., Puig, P., Fabrés, J., Guillén, J., Calafat, A., Canals, M., Heussner, S., Bonnin, J., 2006a. Suspended sediment fluxes and transport processes in the Gulf of Lions submarine canyons. The role of storms and dense water cascading. Mar. Geol. 234, 43-61.

Palanques, A., Martín, J., Puig, P., Guillén, J., Company, J.B., Sardà, F., 2006b. Evidence of sediment gravity flows induced by trawling in the Palamós (Fonera) submarine canyon (northwestern Mediterranean). Deep-Sea Res. Part I Oceanogr. Res. Pap. 53, 201-214.

Palanques, A., Guillén, J., Puig, P., Durrieu de Madron, X., 2008. Storm-driven shelf-to-canyon suspended sediment transport at the southwestern Gulf of Lions. Cont. Shelf Res. 28, 1947-1956.

Palanques, A., Puig, P., Latasa, M., Scharek, R., 2009. Deep sediment transport induced by storms and dense shelf-water cascading in the northwestern Mediterranean basin. Deep-Sea Res. Part I Oceanogr. Res. Pap. 56, 425-434.

Palanques, A., Puig, P., Durrieu de Madron, X., Sànchez-Vidal, A., Pasqual, C., Martín, J., Calafat, A., Heussner, S., Canals, M., 2012. Sediment transport to the deep canyons and open-slope of the western Gulf of Lions during the 2006 intense cascading and open-sea convection period. Prog. Oceanogr. 106, 1-15.

Pasqual, C., Lee, C., Goñi, M., Tesi, T., Sànchez-Vidal, A., Calafat, A., Canals, M., Heussner, S., 2011. Use of organic biomarkers to trace the transport of marine and terrigenous organic matter through the southwestern canyons of the Gulf of Lion. Mar. Chem. 126, 1-12.

Paull, C.K., Mitts, P., Ussler, W., Keaten, R., Greene, H.G., 2005. Trail of sand in upper Monterey Canyon: Offshore California. Bull. Geol. Soc. Am. 117, 1134-1145.

Pierau, R., Henrich, R., Preiß-Daimler, I., Krastel, S., Geersen, J., 2011. Sediment transport and turbidite architecture in the submarine Dakar Canyon off Senegal, NW-Africa. J. African Earth Sci. 60, 196-208.

Pingree, R.D., 1993. Flow of surface waters to the west of the British Isles and in the Bay of Biscay. Deep-Sea Res. Part II Top. Stud. Oceanogr. 40, 369-388.

Pingree, R.D., Le Cann, B., 1990. Structure, strength and seasonality of the slope currents in the Bay of Biscay region. J. Mar. Biol. Assoc. United Kingdom 70, 857-885.

Pingree, R.D., Le Cann, B., 1992. Anticyclonic eddy X91 in the southern Bay of Biscay, May 1991 to February 1992. J. Geophys. Res. Ocean. 97, 14353-14367.

Pingree, R.D., New, A. L., 1989. Downward propagation of internal tidal energy into the Bay of Biscay. Deep-Sea Res. Part A Oceanogr. Res. Pap. 36, 735-758.

Pollard, R.T., Pu, S., 1985. Structure and circulation of the Upper Atlantic Ocean northeast of the Azores. Prog. Oceanogr. 14, 443-462.

Pollard, R.T., Grifftths, M.J., Cunningham, S.A., Read, J.F., Pérez, F.F., Ríos, A.F., 1996. Vivaldi 1991 - A study of the formation, circulation and ventilation of Eastern North Atlantic Central Water. Prog. Oceanogr. 37, 167-192.

Prego, R., Boi, P., Cobelo-García, A., 2008. The contribution of total suspended solids to the Bay of Biscay by Cantabrian Rivers (northern coast of the Iberian Peninsula). J. Mar. Syst. 72, 342-349.

Puig, P., Palanques, A., 1998. Temporal variability and composition of settling particle fluxes on the Barcelona continental margin (Northwestern Mediterranean). J. Mar. Res. 56, 639-654.

Puig, P., Ogston, A.S., Mullenbach, B.L., Nittrouer, C.A., Parsons, J.D., Sternberg, R.W., 2004a. Storm-induced sediment gravity flows at the head of the Eel submarine canyon, northern California margin. J. Geophys. Res. 109, C03019.

Puig, P., Palanques, a., Guillén, J., El Khatab, M., 2004b. Role of internal waves in the generation of nepheloid layers on the northwestern Alboran slope: Implications for continental margin shaping. J. Geophys. Res. C Ocean. 109, 1-11.

Puig, P., Canals, M., Company, J.B., Martín, J., Amblàs, D., Lastras, G., Palanques, A., Calafat, A.M., 2012. Ploughing the deep sea floor. Nature 489, 286-289.

Pusceddu, A., Bianchelli, S., Martín, J., Puig, P., Palanques, A., Masqué, P., Danovaro, R., 2014. Chronic and intensive bottom trawling impairs deep-sea biodiversity and ecosystem functioning. Proc. Nat. Acad. Sc. 111 (24): 8861–8866.

Quaresma, L.S., Vitorino, J., Oliveira, A., da Silva, J., 2007. Evidence of sediment resuspension by nonlinear internal waves on the western Portuguese mid-shelf. Mar. Geol. 246, 123-143.

Ríos, A.F., Pérez, F.F., Fraga, F., 1992. Water masses in the upper and middle North Atlantic Ocean east of the Azores. Deep-Sea Res. Part A Oceanogr. Res. Pap. 39, 645-658.

Ruiz-Villarreal, M., Coelho, H., Díaz del Río, G., Nogueira, J., 2004. Slope current in the Cantabrian: Observations and modeling of seasonal variability and interaction with Aviles Canyon. ICES CM 2004/N:12, 23pp.

Rumín-Caparrós, A., Sànchez-Vidal, A., Calafat, A., Canals, M., Martín, J., Puig, P., Pedrosa-Pàmies, R., 2013. External forcings, oceanographic processes and particle flux dynamics in Cap de Creus submarine canyon, NW Mediterranean Sea. Biogeosciences 10, 3493-3505.

Sánchez, F., González-Pola, C., Druet, M., García-Alegre, A., Acosta, J., Cristobo, J., Parra, S., Ríos, P., Altuna, Á., Gómez-Ballesteros, M., Muñoz-Recio, A., Rivera, J., del Río, G.D., 2014. Habitat characterization of deep-water coral reefs in La Gaviera Canyon (Avilés Canyon System, Cantabrian Sea). Deep-Sea Res. Part II Top. Stud. Oceanogr. 106, 118-140.

Sánchez-Delgado, F., Gómez-Ballesteros, M., Parra-Descalzo, S., Cristobo, J., Serrano-López, A., Druet-Vélez, M., García-Alegre-Garralda, A., Rodríguez-Cabello-Ródenas, M.C., Preciado-Ramírez, M.I., Tello-Antón, M.O., Punzón-Merino, A.M., Blanco-Giner, M.Á., Ríos, P., Frutos-Parralejo, M.I., González-Pola, C., Acosta-Yepes, J., Rivera, J., 2014. Caracterización ecológica del área marina del sistema de cañones submarinos de Avilés. Informe final área LIFE+ INDEMARES (LIFE07/NAT/E/000732), 243 pp. Instituto Español de Oceanografía. Coordinación: Fundación Biodiversidad, Madrid.

Sànchez-Vidal, A., Canals, M., Calafat, A.M., Lastras, G., Pedrosa-Pàmies, R., Menéndez, M., Medina, R., Company, J.B., Hereu, B., Romero, J., Alcoverro, T., 2012. Impacts on the deep-sea ecosystem by a severe coastal storm. PLoS One 7, e30395.

Schmidt, S., Howa, H., Mouret, A., Lombard, F., Anschutz, P., Labeyrie, L., 2009. Particle fluxes and recent sediment accumulation on the Aquitanian margin of Bay of Biscay. Cont. Shelf Res. 29, 1044-1052.

Schmidt, S., Howa, H., Diallo, A., Martín, J., Cremer, M., Duros, P., Fontanier, C., Deflandre, B., Metzger, E., Mulder, T., 2014. Recent sediment transport and deposition in the Cap-Ferret Canyon, South-East margin of Bay of Biscay. Deep-Sea Res. Part II Top. Stud. Oceanogr. 104, 134-144.

Serpette, A., Le Cann, B., Colas, F., 2006. Lagrangian circulation of the North Atlantic Central Water over the abyssal plain and continental slopes of the Bay of Biscay: description of selected mesoscale features. Sci. Mar. 70, 27-42.

Shepard, F.P., 1981. Submarine canyons: multiple causes and long-time persistence. Am. Assoc. Pet. Geol. Bull. 65, 1062-1077.

Shepard, F.P., Marshall, N.F., McLoughlin, P.A., Sullivan, G.G., 1979. Currents in submarine canyons and other seavalleys. AAPG St. Geol. 8, 173 p.

Smith, S.D., 1988. Coefficients for sea surface wind stress, heat flux, and wind profiles as a function of wind speed and temperature. J. Geophys. Res. 93, 15467-15472.

Somavilla, R., González-Pola, C., Rodríguez, C., Josey, S. A., Sánchez, R. F., Lavín, A., 2009. Large changes in the hydrographic structure of the Bay of Biscay after the extreme mixing of winter 2005. J. Geophys. Res. 114, 1-14.

Stabholz, M., Durrieu de Madron, X., Canals, M., Khripounoff, A., Taupier-Letage, I., Testor, P., Heussner, S., Kerhervé, P., Delsaut, N., Houpert, L., Lastras, G., Dennielou, B., 2013. Impact of open-ocean convection on particle fluxes and sediment dynamics in the deep margin of the Gulf of Lions. Biogeosciences 10, 1097-1116.

Stenseth, N.C., Llope, M., Anadón, R., Ciannelli, L., Chan, K.-S., Hjermann, D.Ø., Bagøien, E., Ottersen, G., 2006. Seasonal plankton dynamics along a cross-shelf gradient. Proc. Biol. Sci. 273, 2831-8.

Taylor, J.R., Sarkar, S., 2008. Stratification effects in a bottom Ekman layer. J. Phys. Oceanogr. 38, 2535-2555.

Tyler, P., Amaro, T., Arzola, R., Cunha, M.R., de Stigter, H., Gooday, A., Huvenne, V., Ingels, J., Kiriakoulakis, K., Lastras, G., Masson, D., Oliveira, A., Pattenden, A., Vanreusel, A., Van Weering, T., Vitorino, J., Witte, U., Wolff, G., 2009. Europe's Grand Canyon: Nazaré Submarine Canyon. Oceanography 22, 46-57.

Ulses, C., Estournel, C., Bonnin, J., Durrieu de Madron, X., Marsaleix, P., 2008a. Impact of storms and dense water cascading on shelf-slope exchanges in the Gulf of Lion (NW Mediterranean). J. Geophys. Res. 113, 1-18.

Ulses, C., Estournel, C., Durrieu de Madron, X., Palanques, A., 2008b. Suspended sediment transport in the Gulf of Lions (NW Mediterranean): Impact of extreme storms and floods. Cont. Shelf Res. 28, 2048-2070.

van Aken, H.M., 2000a. The hydrography of the mid-latitude Northeast Atlantic Ocean. I: The deep water masses. Deep-Sea Res. Part I Oceanogr. Res. Pap. 47, 757-788.

van Aken, H.M., 2000b. The hydrography of the mid-latitude Northeast Atlantic Ocean. II: The intermediate water masses. Deep-Sea Res. Part I Oceanogr. Res. Pap. 47, 789-824.

van Aken, H.M., 2001. The hydrography of the mid-latitude Northeast Atlantic Ocean - Part III: The subducted thermocline water mass. Deep-Sea Res. Part I Oceanogr. Res. Pap. 48, 237-267.

van Weering, T.C.E., de Stigter, H.C., Boer, W., de Haas, H., 2002. Recent sediment transport and accumulation on the NW Iberian margin. Prog. Oceanogr. 52, 349-371.

Vetter, E.W., 1994. Hotspots of benthic production. Nature 372, 47.

Vetter, E.W., Dayton, P.K., 1998. Macrofaunal communities within and adjacent to a detritus-rich submarine canyon system. Deep-Sea Res. Part II Top. Stud. Oceanogr. 45, 25-54.

Vetter, E.W., Smith, C.R., De Leo, F.C., 2010. Hawaiian hotspots: enhanced megafaunal abundance and diversity in submarine canyons on the oceanic islands of Hawaii. Mar. Ecol. 31, 183-199.

Walsh, I.D., Gardner, W.D., 1992. A comparison of aggregate profiles with sediment trap fluxes. Deep-Sea Res. Part A Oceanogr. Res. Pap. 39, 1817-1834.

Xu, J., Noble, M., Eittreim, S.L., Rosenfeld, L.K., Schwing, F.B., Pilskaln, C.H., 2002. Distribution and transport of suspended particulate matter in Monterey Canyon, California. Mar. Geol. 181, 215-234.

Xu, J.P., Swarzenski, P.W., Noble, M., Li, A.-C., 2010. Event-driven sediment flux in Hueneme and Mugu submarine canyons, southern California. Mar. Geol. 269, 74-88.

Figure captions

Figure 1. Shaded relief bathymetric map of the Avilés submarine canyon and surrounding shelf, slope and deep basin. The location of the El Corbiro Canyon (ECC) and the La Gaviera Canyon (LGC) are indicated. Location of moorings (white dots), Cabo Peñas coastal buoy (blue dot) and WANA point 1053075 (green dot) are also presented. Dashed black lines mark the boundaries of the upper and middle canyon course. The black box includes La Vallina branches illustrated in Figure 2. Land topography from the NASA's Lance rapid response MODIS satellite true colour images. Depth is in meters. The top right map represents the NE Atlantic Ocean with the Cantabrian margin (CM) forming the southern bound of the Bay of Biscay (BoB).

Figure 2. Shaded relief images of tributaries entering the Avilés Canyon from its western flank. (a) General view of tributaries incised in the western flank of the Avilés Canyon middle course and lower upper course. (b) Zoom in of La Vallina westernmost branch showing a dominantly smoothened relief. (c) Zoom in of a set of La Vallina branches showing a smoothened relieve mainly of the right flanks of shelf-incised segments. Note the presence of some flank gullies locally forming closely spaced sets. See Figure 1 for location.

Figure 3. (a) Water discharge of Nalón River encompassing the studied annual cycle (March 2012-April 2013). (b) Temporal evolution of monthly mean Chlorophyll-a concentration centred over the Avilés Canyon. (c) Wind direction at Cabo Peñas coastal buoy with dots representing the direction from which the wind is blowing. (d) Wind speed. (e) Wave direction at Cabo Peñas coastal buoy with dots representing the direction from which the waves are arriving. (f) Significant wave height (Hs) at Cabo Peñas Seawatch coastal buoy. (g) Current direction measured by the currentmeter installed in the Cabo Peñas buoy at 3 m depth. (h) Current speed at 3 m depth measured by the currentmeter of the Cabo Peñas buoy. Note that wind direction and speed records start about one month later (in grey data from the WANA point 1053075, see location in Fig. 1) than wave and current data due to a technical failure of the buoy's meteorological sensors. Shaded areas highlight specific events discussed in the text.

Figure 4. Total mass fluxes (TMF) and lateral fluxes (LF) in the mooring stations deployed within the Avilés Canyon and on the open upper slope to the west. (a) TMFs at the open upper slope station WS1200 (near-bottom) west of the canyon. (b) TMFs in

the middle course station for levels AC2000B (black stepped line, near-bottom) and AC2000T (grey stepped line, mid-water). (c) TMFs in the lowermost canyon course station AC4700 (near-bottom). (d) and (e) LFs at WS1200 (near-bottom) and AC2000B (near-bottom) in black. The grey dashed line represents re-sampled lateral fluxes adjusted to time steps equal to the sampling interval of the sediment traps.

Figure 5. Temporal variability of the main components of the settling particle fluxes collected by the sediment traps in the mooring stations deployed within and on the open slope west of Avilés Canyon during the studied annual cycle (March 2012-April 2013). (a) Lithogenics. (b) $CaCO_3$. (c) Organic matter (black dots), molar nitrogen:organic carbon ratios (N:C, red dots). (d) Opal. Codes of mooring stations and levels correspond to those in figures 1 and 5, and in Table 1.

Figure 6. Lance rapid response MODIS satellite true colour images from the NASA Earth Observing System Data and Information System (EOSDIS) with the shaded relief bathymetry of the Avilés Canyon and adjacent open slope as background layer. White dots indicate the mooring sites. Dashed white lines follow the outer limit of coast-derived sediment plumes at sea surface. (a) Image from 21 January 2013 illustrating plume dispersal under a westward surface circulation. (b) Image from 4 May 2013 illustrating plume dispersal under an eastward surface circulation.

Figure 7. MODIS-based net primary production maps (mg C m^{-2} d^{-1}) showing the development of phytoplanktonic blooms that occurred in spring 2012 and 2013. Black squares correspond to the area shown in figure 1 and white dots indicate mooring locations.

Figure 8. Time series of upwelling index (UI) during (a) January to April 2012, and (b) January to April 2013. The grey line represents data from the WANA point 1053075. Shaded areas highlight specific events discussed in the text. Note that albeit we do not have particle flux data during January and February 2012, data on UI during such months have been included to note the more persistent upwelling favourable conditions during winter 2013 than during the previous winter.

Figure 9. Current speed (black line) and de-tided current speed (green line) over (a) the continental slope west of Avilés Canyon at 1200 m depth near-bottom (WS1200); (b) the Avilés Canyon middle course (AC2000T) at mid-water depth (1200 m); and (c)

the Avilés Canyon (AC2000B) middle course near-bottom. The vertical grey dashed line marks the boundary between the two observational periods (see section 3.3).

Figure 10. Progressive vector diagram built after near-bottom raw (non-filtered) currents recorded at the location of AC2000B (near-bottom) in Avilés Canyon from 1 April 2012 to 31 May 2012. The position of the mooring stations in the middle canyon (AC2000) and the lowermost canyon (AC4700) is indicated with black dots.

Figure 11. Scheme illustrating wind regimes and associated processes including sediment transport (a) during spring and summer, when easterly winds induce a westward circulation and favour the advection of coast-derived sea surface sediment plumes towards Avilés Canyon and its adjacent open slope, and (b) during autumn and winter, when westerly winds induce and eastward circulation pushing sea surface sediment plumes against the shoreline, i.e. away from the canyon head and upper course. Note, however, that the bottom Ekman transport is directed offshore (see section 5.1).
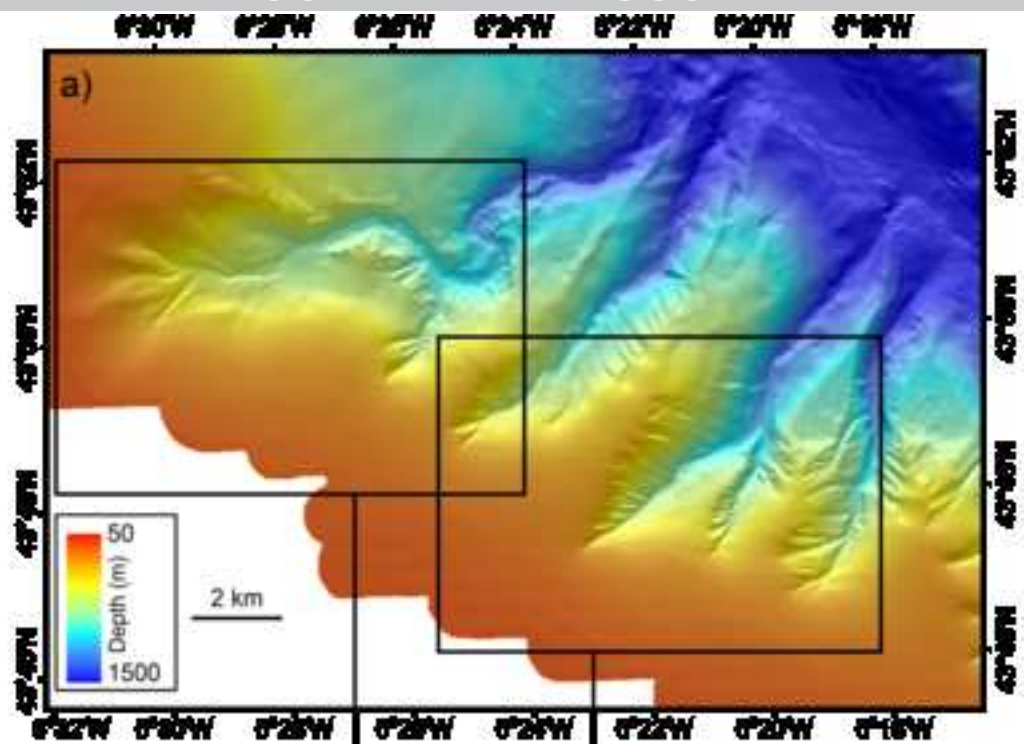
Figure 1
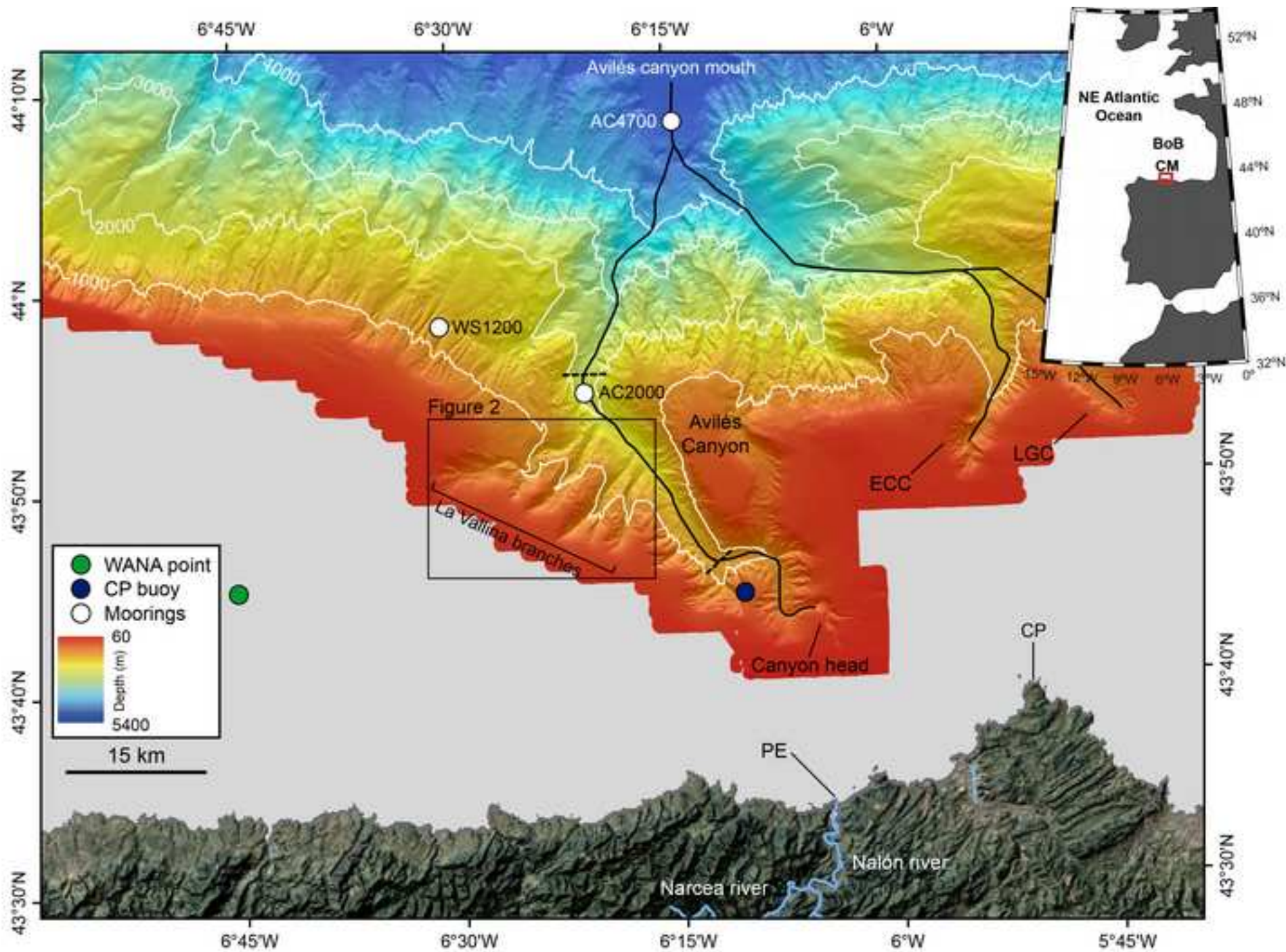
Figure 2

a)

Depth (m)
50
1500

2 km

b)

Shelf-indented smoothened flanks

1 km

c)

Smoothened right flank
(shelf-indented segment)

Closely spaced gullies

1 km
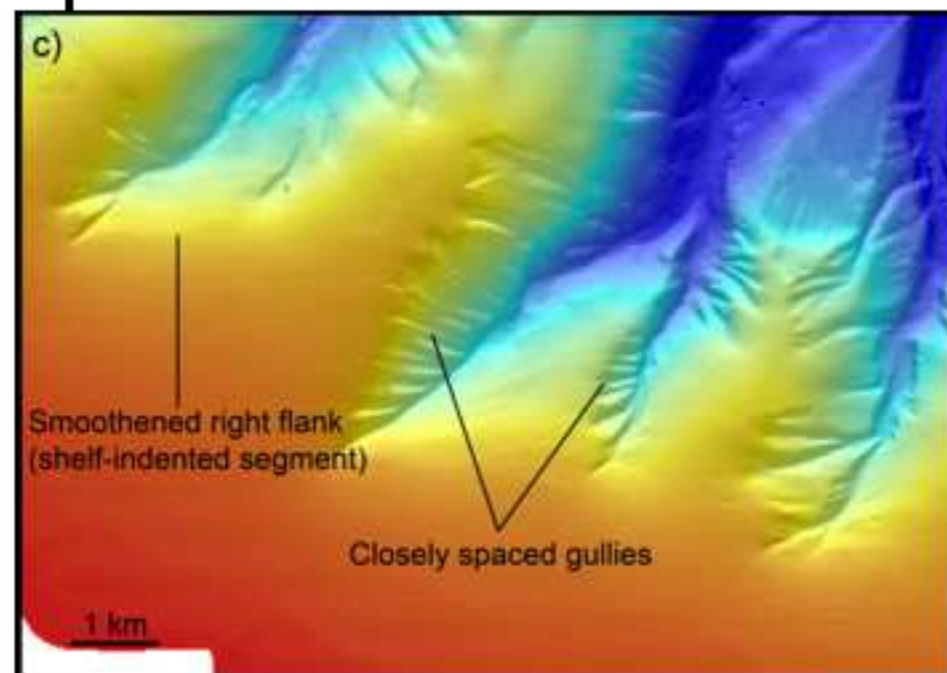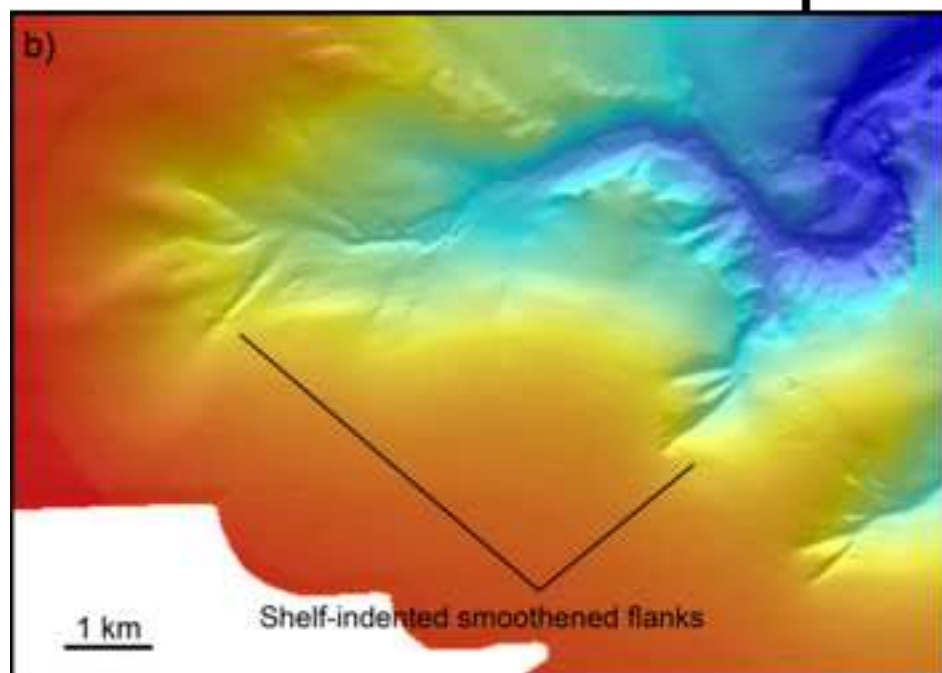
Figure 3

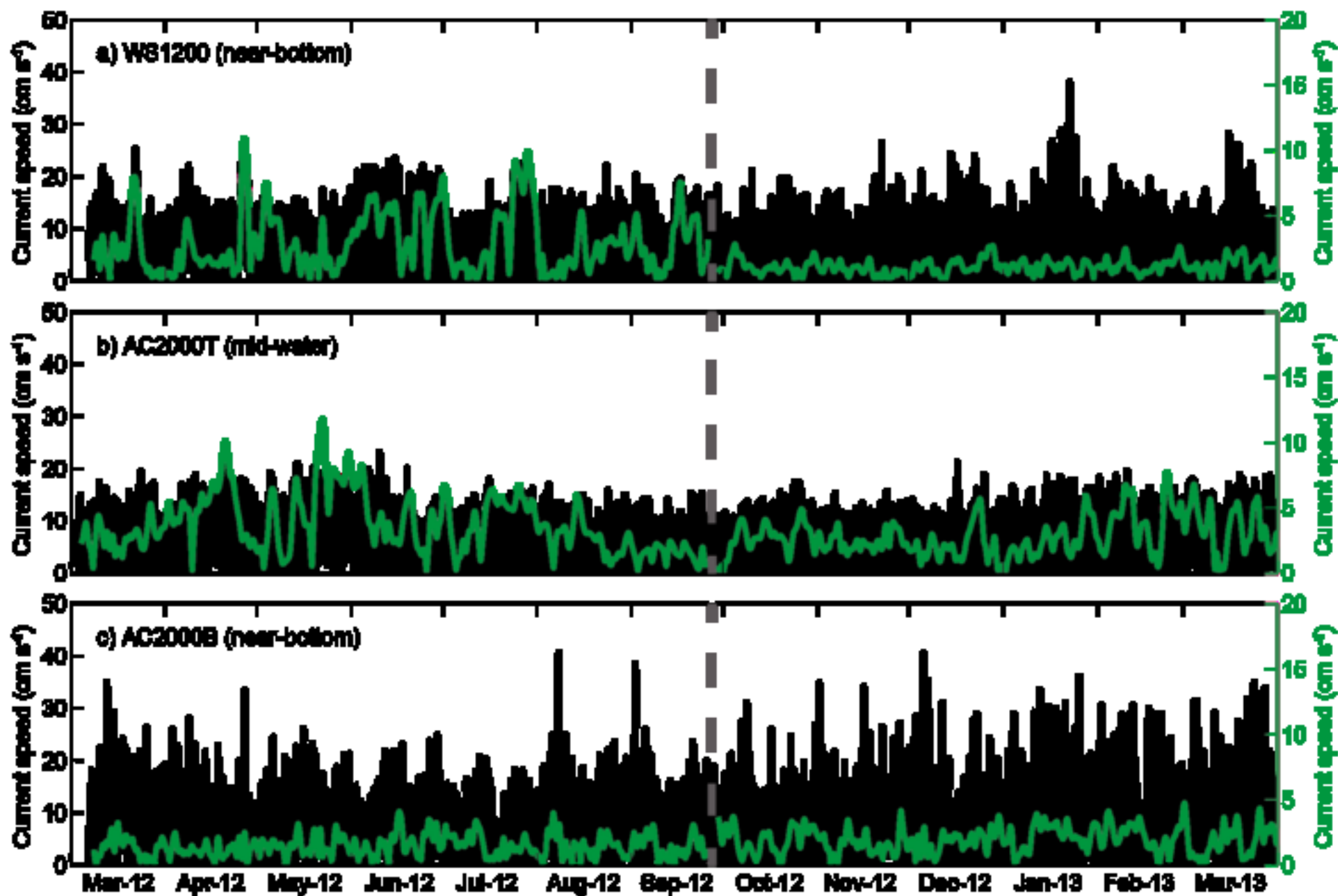**Figure 5**
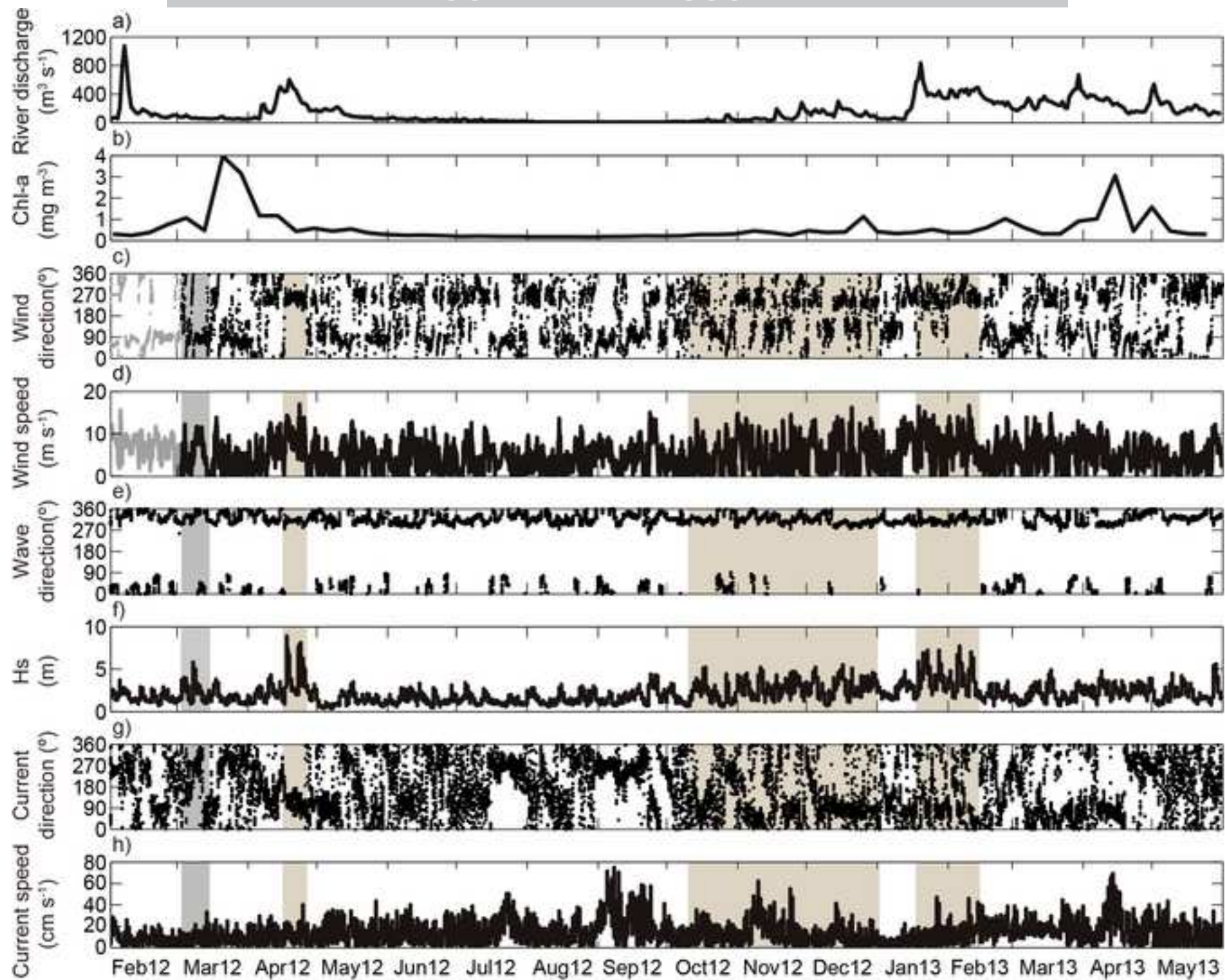
Figure 6

Figure 7

Figure 8
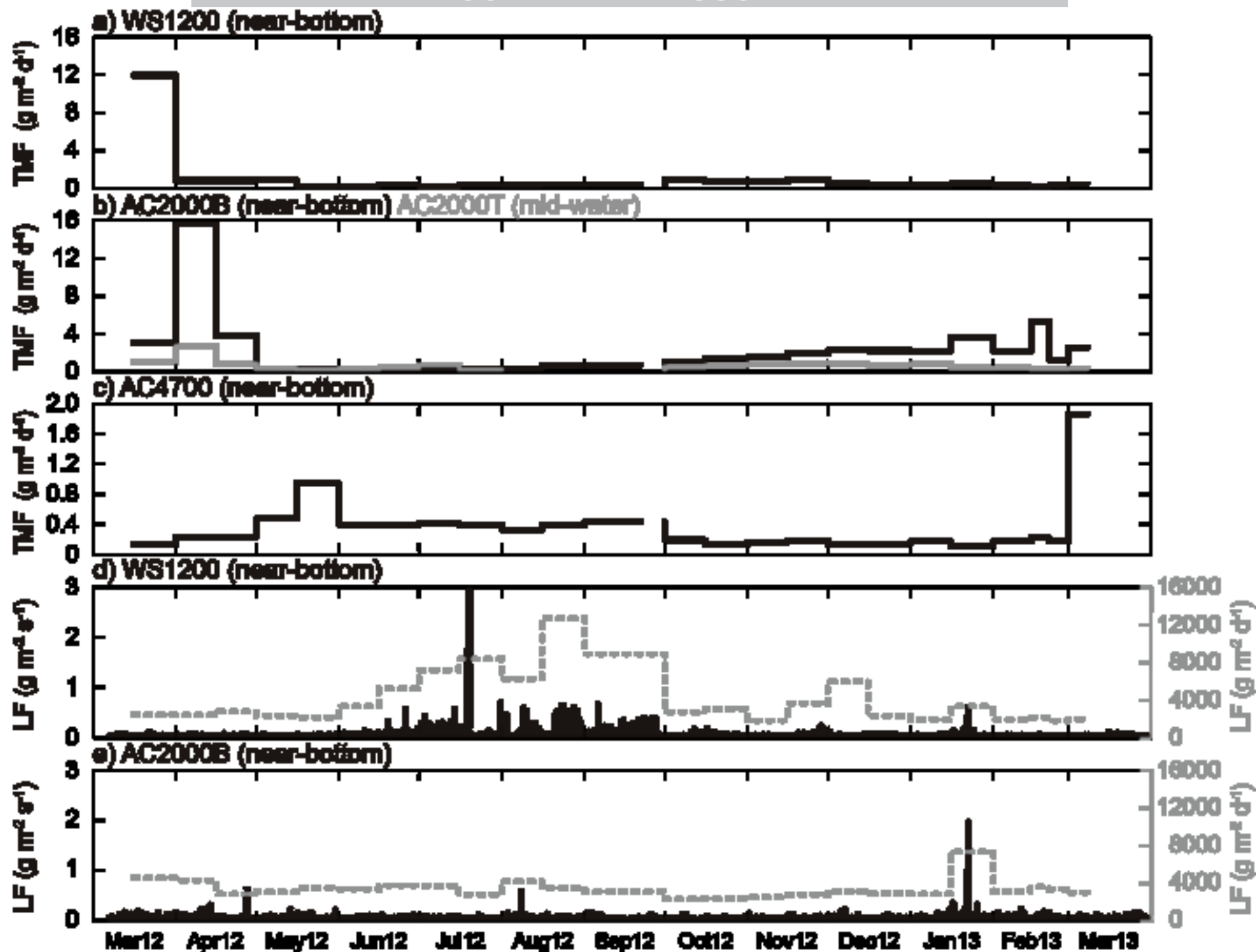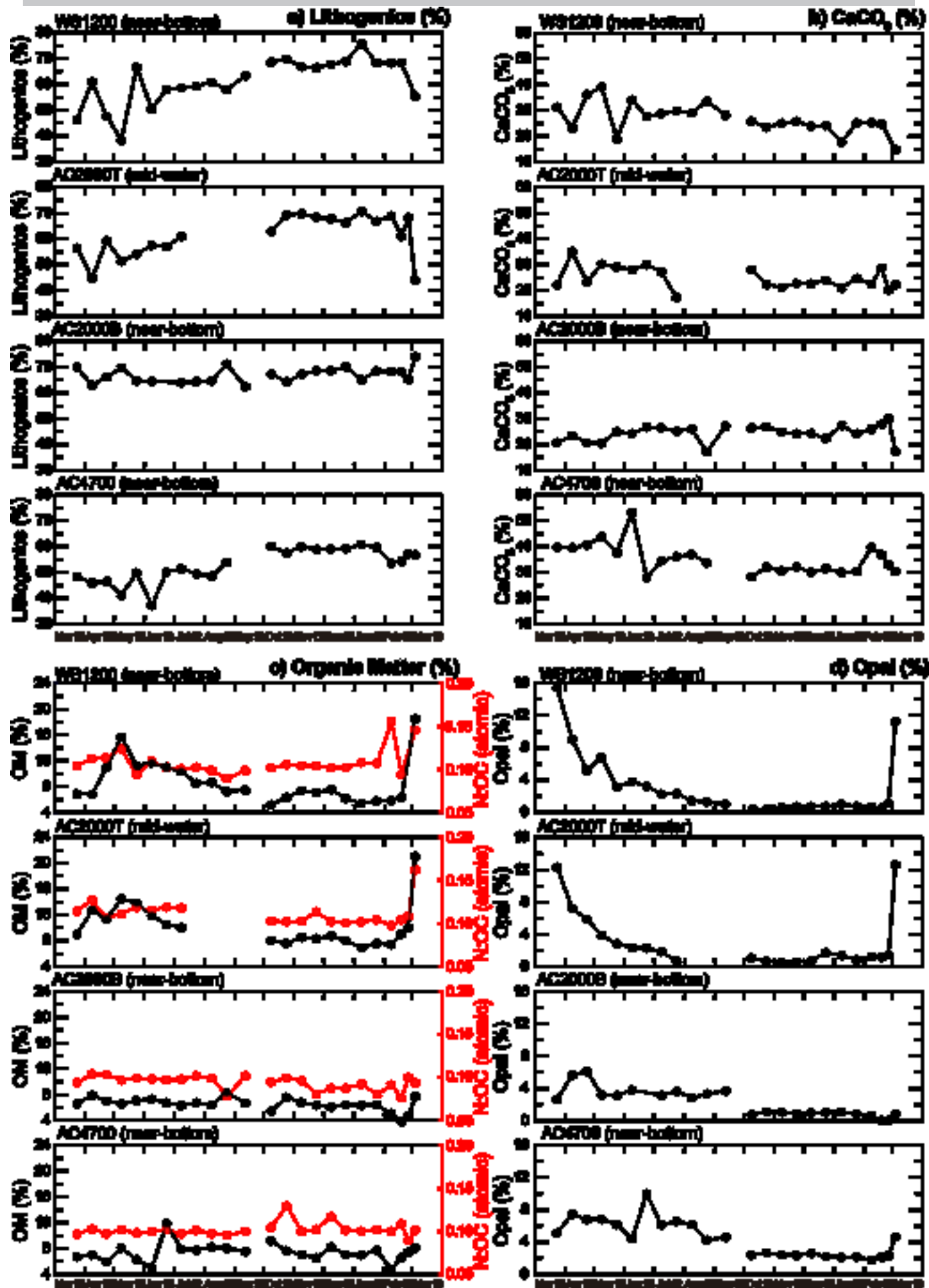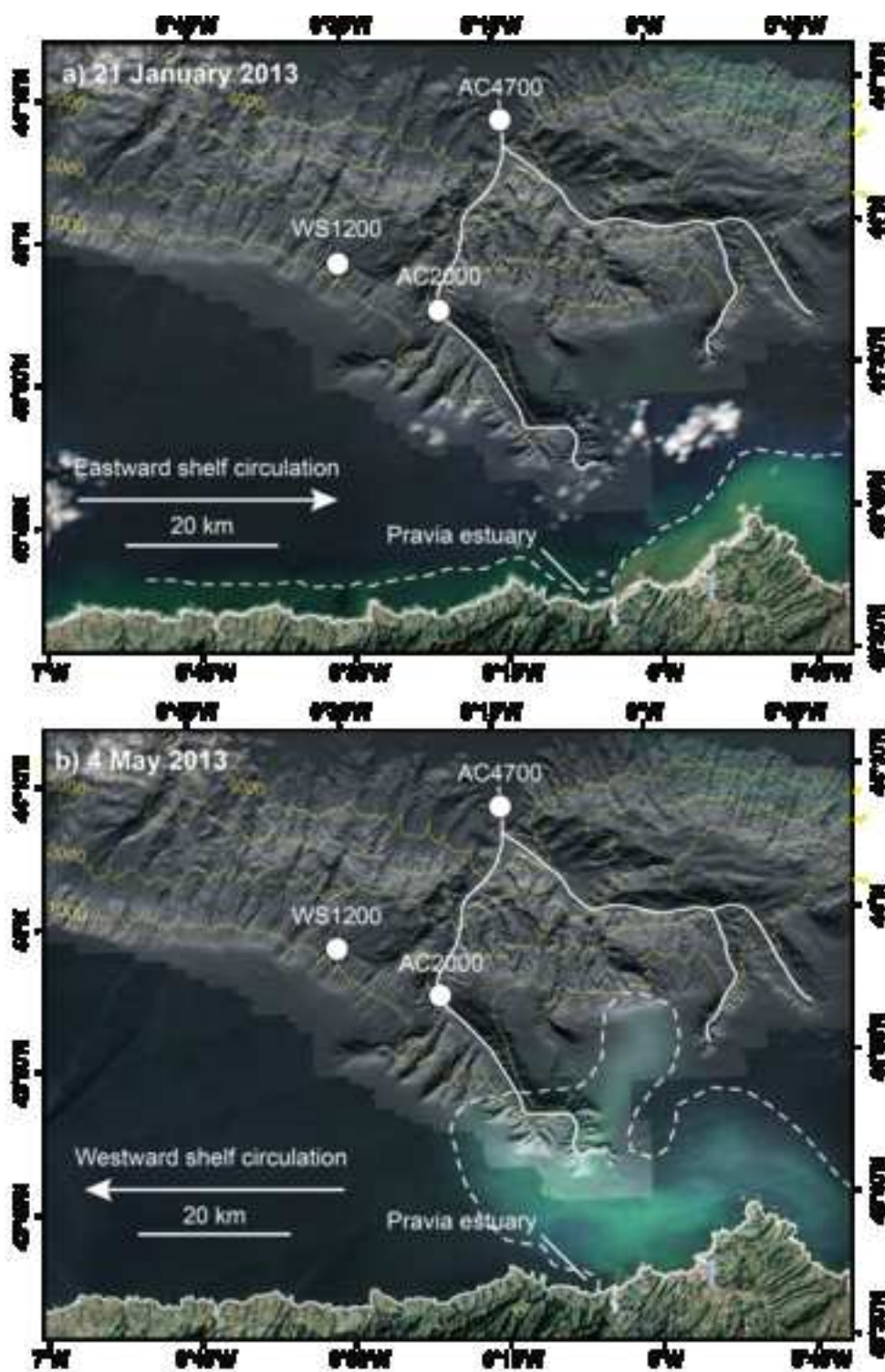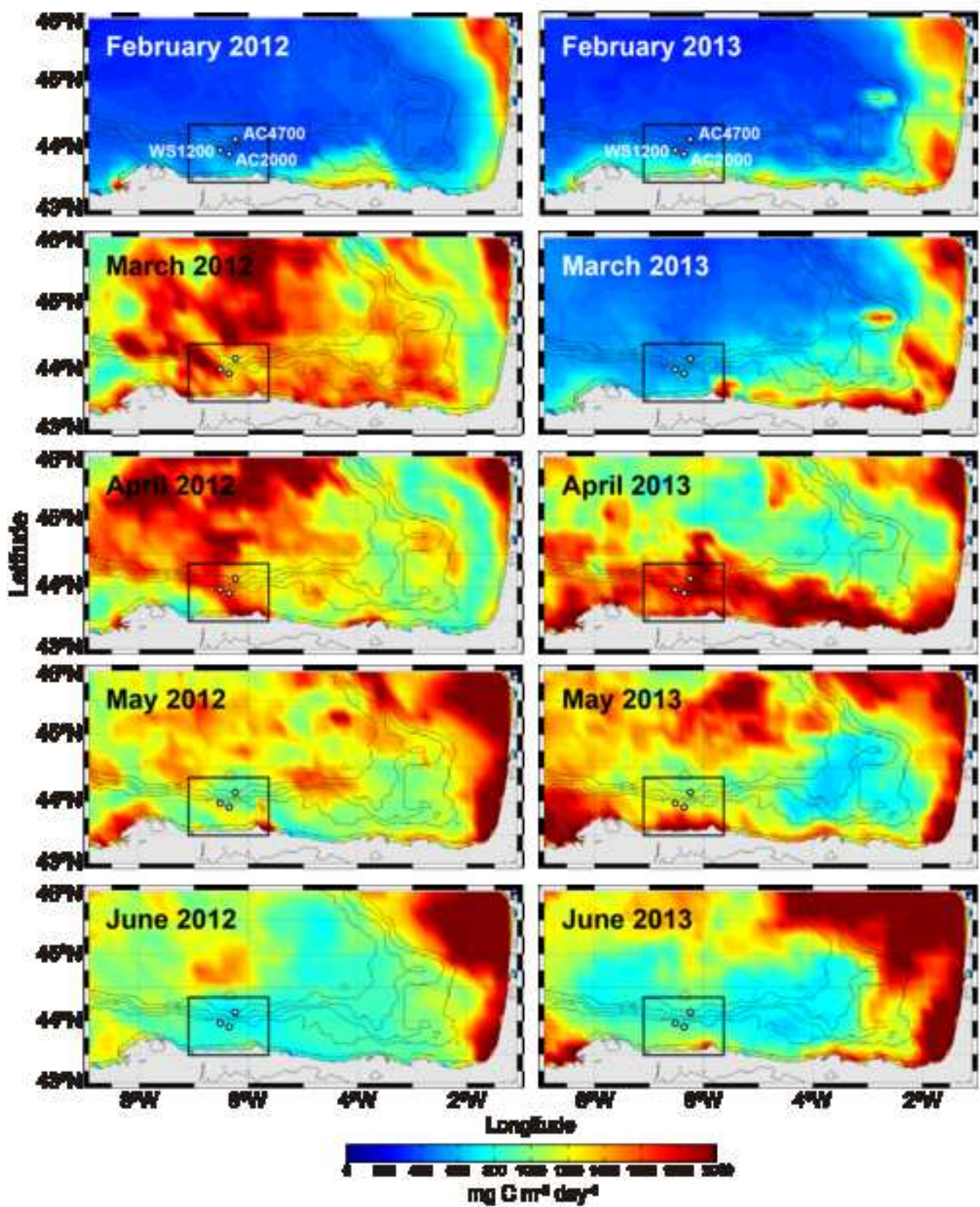
Figure 9

Figure 10

Figure 11
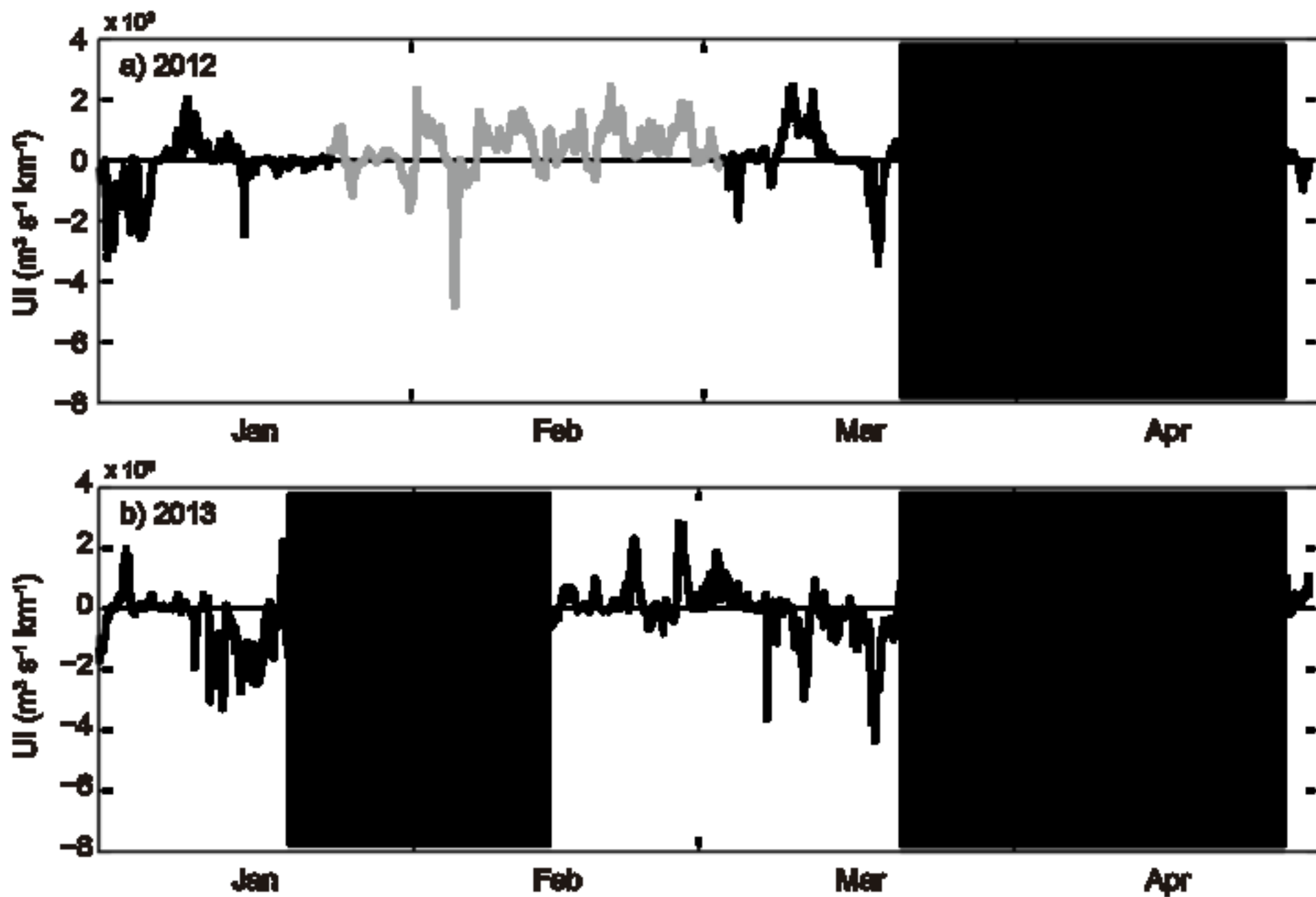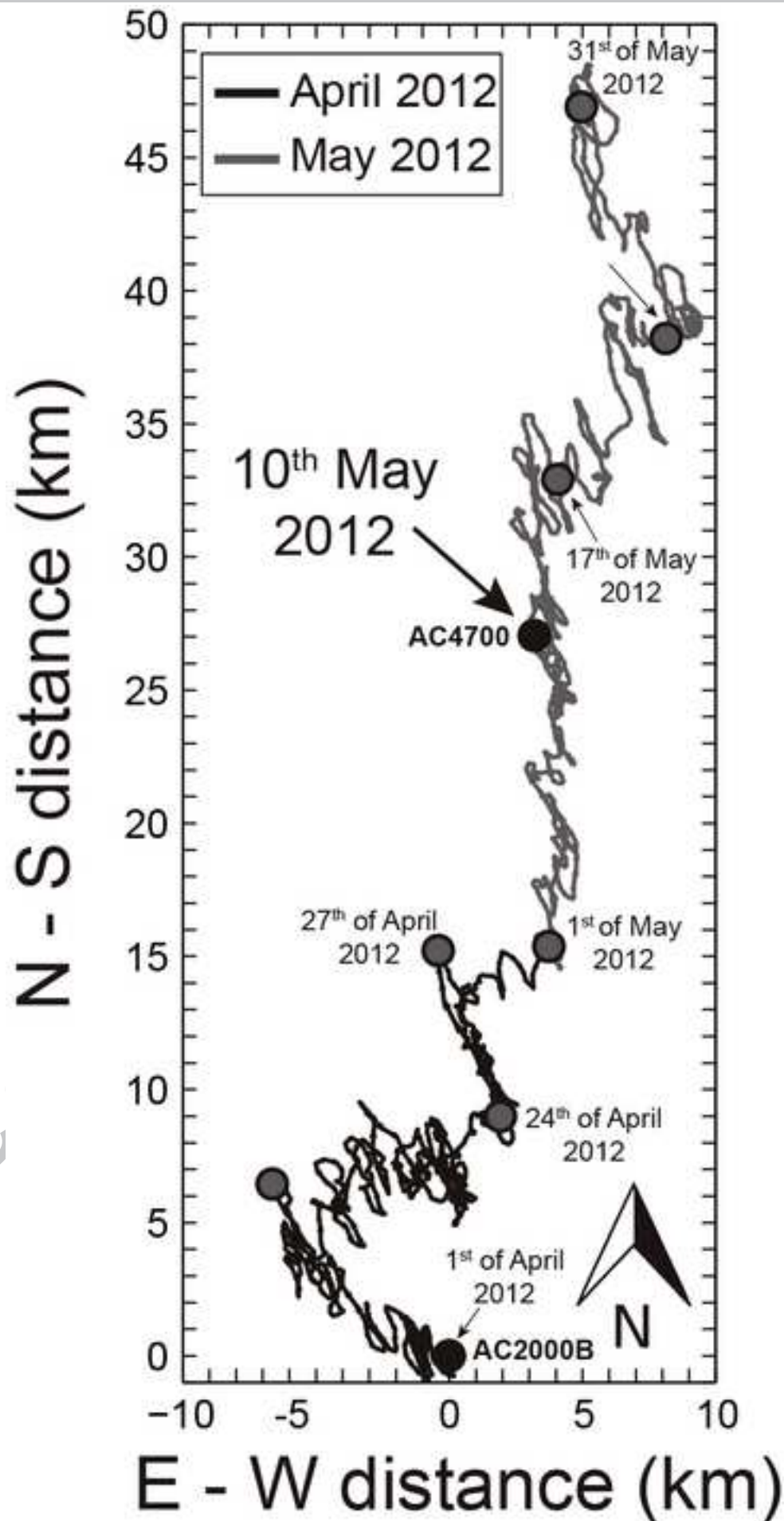
a) Upwelling season (spring - summer)

Easterly winds

N

CP

P

AC
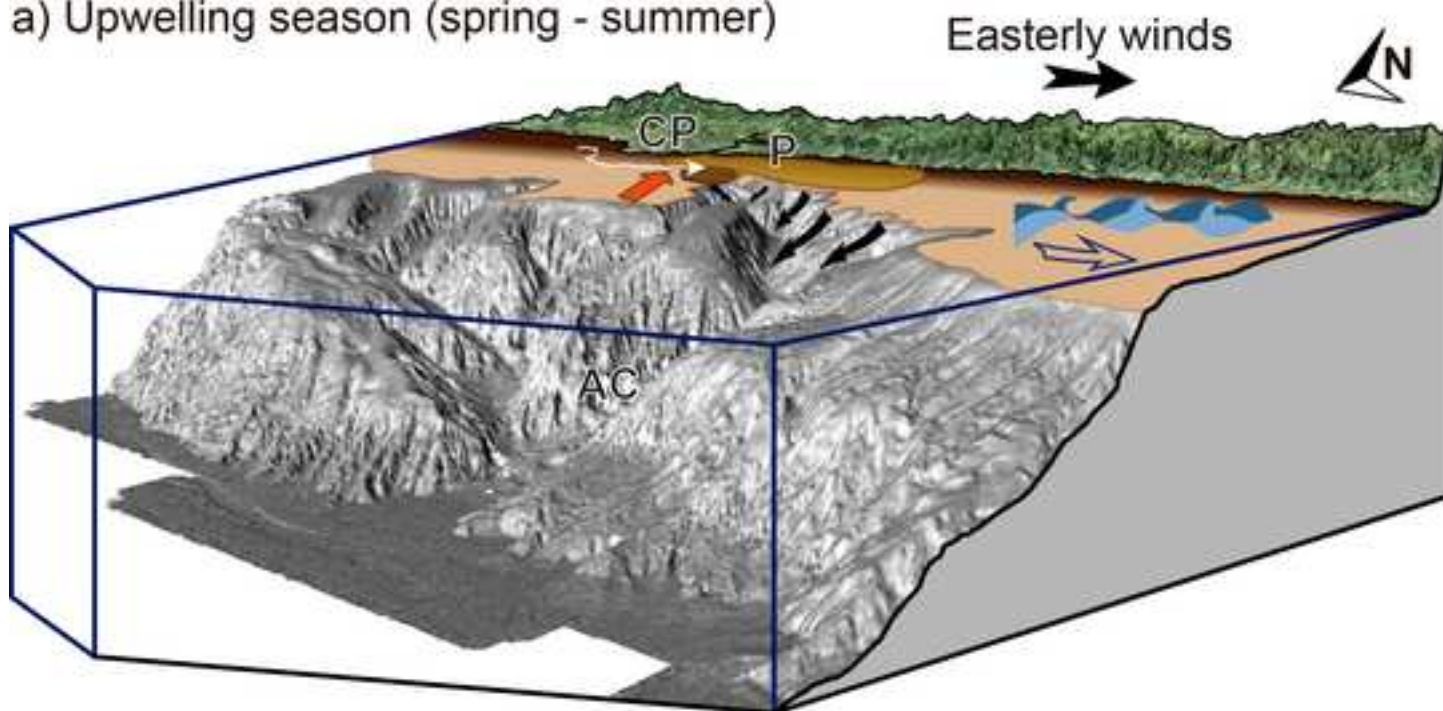
b) Downwelling season (autumn - winter)

Westerly winds

N

CP

P

AC
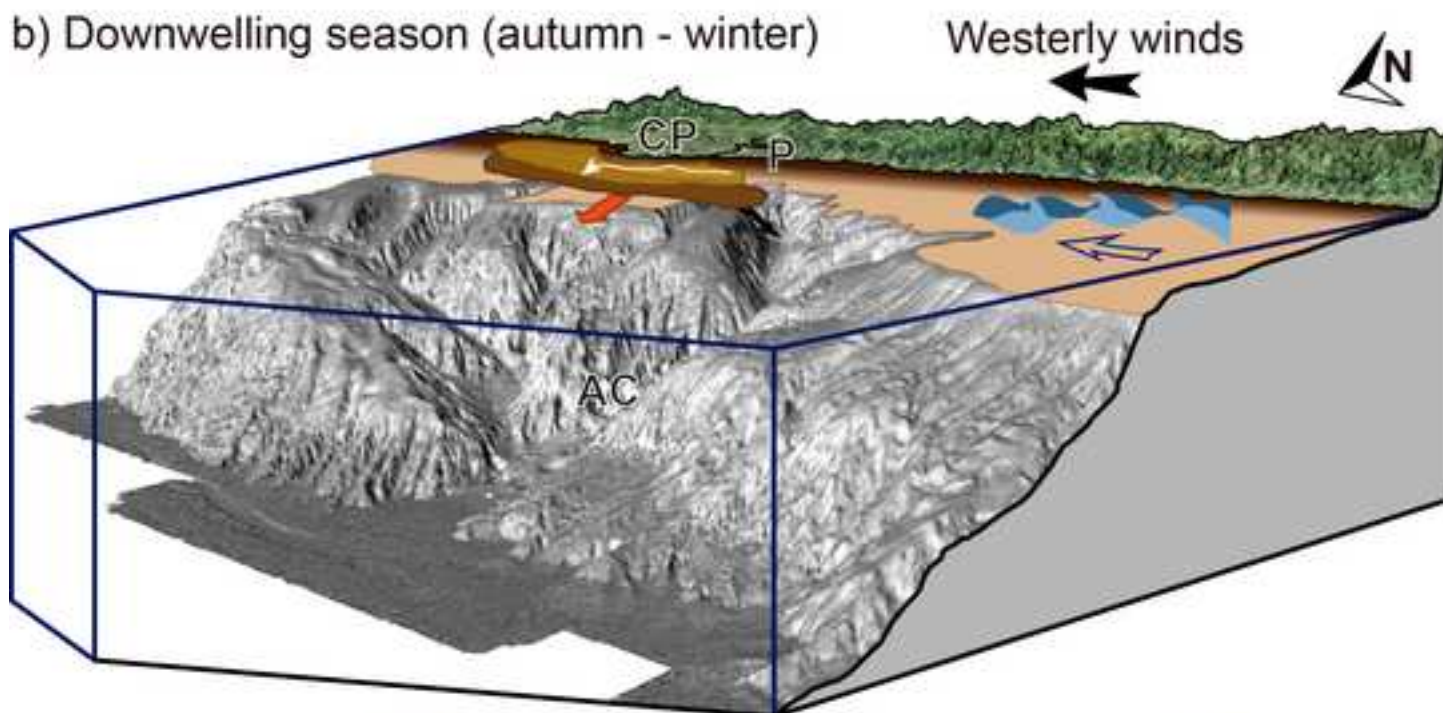
AC: Avilés Canyon
CP: Cabo Peñas
P: Pravia estuary

Riverine particulate matter

Freshly deposited sediment

Shelf resuspended sediment

Main shelf current

Inner shelf current acceleration

Bottom Ekman transport

Channalized sediment transport

Waves

Table captions

Table 1. Average annual fluxes (g m^{-2} d^{-1}) and relative contribution of each of the major constituents to particle fluxes in the Avilés Canyon and adjacent open slope to the west.

Station	Water Depth	Meters above the bottom	Meters below surface	TWF	Lithogenic		CaCO$_3$		OM		Opal	
					%	Flux	%	Flux	%	Flux	%	Flux
	(m)	(m)	(m)	(g m^{-2} d^{-1})		(g m^{-2} d^{-1})		(g m^{-2} d^{-1})		(g m^{-2} d^{-1})		(g m^{-2} d^{-1})
WS1200	1200	46	1154	0.99	61.42	0.54	26.78	0.30	8.62	0.078	3.09	0.09
AC2000T (mid-water)	2000	822	1178	0.43	61.32	0.30	24.93	0.14	10.25	0.05	3.00	0.021
AC2000B (near-bottom)	2000	46	1954	1.98	66.98	1.37	24.42	0.47	6.52	0.14	2.20	0.07
AC4700	4700	46	4654	0.33	53.05	0.17	35.19	0.12	7.42	0.025	4.36	0.017

Table 2. Results of the three-way ANOVA performed on total mas fluxes (TMFs). The sum of the squares (SS), the degree of freedom (DF), the relative contribution to the overall variability of TMFs of each of the factors considered, and the F value and its probability "p" are presented.

Factors	SS	DF	% Total variability	F	p
Trap depth	5.22E+08	2	8	134.23	<0.001
Month of collection	1.35E+09	11	21	134.23	<0.001
Trap depth * Month of collection	1.99E+09	22	31	46.60	<0.001
Residual (unexplained)	2.53E+09	1303	40		
Total	7.67E+09	1338	100		

Table 3. Overall cross-correlation coefficients between time series of external forcings and total mas fluxes during the studied period. Each time lag unit corresponds to 15 days.

Station		Wind speed	Wave height	Total river discharge
WS1200	Correlation coefficient	0.458	0.459	0.507
		(lag 2)	(lag 2)	(lag 4)
AC2000T (mid-water)	Correlation coefficient	0.716	0.722	0.681
		(lag 1)	(lag 1)	(lag 3)
AC2000B (near-bottom)	Correlation coefficient	0.626	0.639	0.667
		(lag 1)	(lag 1)	(lag 3)
AC4700 (near-bottom)	Correlation coefficient	0.73	0.68	0.69
		(lag 0)	(lag -3)	(lag -3)

Highlights

- Avilés Canyon is one of the largest submarine canyons in Europe.

- Total mass fluxes are dominated by river-sourced lithogenics (53-67%).

- Biological inputs account in average for more than 30% of the total mass flux.

- Wind regime, storms and tides drive sediment dynamics in the canyon.

- No seasonal signal is found in mass fluxes in the middle-lower canyon reaches.